PHILOSOPHICAL TRANSACTIONS A

royalsocietypublishing.org/journal/rsta

Review

**Cite this article:** Brinker K, Dvorsky M, Al Qaseer MT, Zoughi R. 2020 Review of advances in microwave and millimetre-wave NDT&E: principles and applications. *Phil. Trans. R. Soc. A* **378**: 20190585.
http://dx.doi.org/10.1098/rsta.2019.0585

Accepted: 16 April 2020

One contribution of 15 to a theme issue 'Advanced electromagnetic non-destructive evaluation and smart monitoring'.

**Subject Areas:**
electrical engineering, electromagnetism

**Keywords:**
microwave NDT, millimetre wave NDT, imaging, sensing, materials characterization, surface crack detection

**Author for correspondence:**
Katelyn Brinker
e-mail: brinker@iastate.edu

# Review of advances in microwave and millimetre-wave NDT&E: principles and applications

Katelyn Brinker, Matthew Dvorsky, Mohammad Tayeb Al Qaseer and Reza Zoughi

Department of Electrical and Computer Engineering (ECpE), Center for Nondestructive Evaluation (CNDE), Iowa State University, Ames, IA 50011, USA

KB, 0000-0002-8782-3979; MD, 0000-0001-7522-092X; MTAQ, 0000-0001-6003-5078; RZ, 0000-0001-9421-1551

Microwave and millimetre-wave non-destructive testing and evaluation (NDT&E) has a long history dating back to the late 1950s (Bahr 1982 *Microwave non-destructive testing methods*; Zoughi 2000 *Microwave Non-destructive testing and evaluation principles*; Feinstein 1967 *Surface crack detection by microwave methods*; Ash 1973 In *3rd European Microwave Conference*; Auld 1981 *Phys. Technol.* **12**, 149–154; Case 2017 *Mater. Eval.* **75**). However, sustained activities in this field date back to the early 1980s (Zoughi 1995 *Res. Nondestr. Eval.* **7**, 71–74; Zoughi 2018 *Mater. Eval.* **76**, 1051–1057; Kharkovsky 2007 *IEEE Instrumentation & Measurement Magazine* **10**, 26–38). Owing to various limitations associated with using microwaves and millimetre waves for NDT&E, these techniques did not see much utility in the early days. However, with the advent and prevalence of composite materials and structures, in a wide range of applications, and technological advances in high-frequency component design and availability, these techniques are no longer considered as 'emerging techniques' (Zoughi 2018 *Mater. Eval.* **76**, 1051–1057; Schull 2002 *Nondestructive evaluation: theory, techniques, and applications*). Currently, microwave and millimetre-wave NDT&E is a rapidly growing field and has been more widely acknowledged and accepted by practitioners over the last 25+ years (Case 2017 *Mater. Eval.* **75**; Bakhtiari 1994 *IEEE Trans. Microwave Theory Tech.* **42**, 389–395; Bakhtiari 1993 *Mater. Eval.* **51**, 740–743; Bakhtiari 1993 *IEEE Trans. Instrum. Meas.*

THE ROYAL SOCIETY PUBLISHING

**42**, 19–24; Ganchev 1995 *IEEE Trans. Instrum. Meas.* **44**, 326–328; Bois 1999 *IEEE Trans. Instrum. Meas.* **48**, 1131–1140; Ghasr 2009 *IEEE Trans. Instrum. Meas.* **58**, 1505–1513). Microwave non-destructive testing was recently recognized and designated by the American Society for Nondestructive Testing (ASNT) as a 'Method' on its own (Case 2017 *Mater. Eval.* **75**). These techniques are well suited for materials characterization; layered composite inspection for thickness, disbond, delamination and corrosion under coatings; surface-breaking crack detection and evaluation; and cure-state monitoring in concrete and resin-rich composites, to name a few. This work reviews recent advances in four major areas of microwave and millimetre-wave NDT&E, namely materials characterization, surface crack detection, imaging and sensors. The techniques, principles and some of the applications in each of these areas are discussed.

This article is part of the theme issue 'Advanced electromagnetic non-destructive evaluation and smart monitoring'.

## 1. Introduction

The field of non-destructive testing and evaluation (NDT&E) involves the development and employment of techniques to non-invasively inspect and characterize materials and structures without inhibiting their usefulness or causing irreversible damage [1,2]. An NDT&E system typically consists of a transducer that produces the interrogating signal and receives the scattered signal after it has interacted with the material under test (MUT) and a detector that measures the received signal. Proper analysis of the measured signal provides information about the material and structural 'state' of the MUT. An NDT&E system can then be further described by the type of interrogating signal it produces, the materials it inspects and other metrics such as resolution and dynamic range [1,3].

The microwave and millimetre-wave frequency range spans from approximately 300 MHz to 300 GHz, corresponding to wavelengths of 1 m and 1 mm, respectively [1,4,5]. Figure 1 shows where these considered methods lie on the electromagnetic spectrum with respect to other common NDT&E methods. In general, as frequency increases 'resolution' increases and the feature size that can be detected becomes smaller, meaning that microwave and millimetre-wave techniques can detect relatively small anomalies and flaws [1,4–6].

These techniques are well suited for inspecting dielectric materials, since waves not only readily penetrate these materials, but are also sensitive to changes in their dielectric properties [1,5–7]. On the other hand, waves at these frequencies do not penetrate highly conductive materials (i.e. metals or carbon-based composites). This is due to the limited skin depth, which is a figure-of-merit that describes the extent to which waves penetrate and decay in conductors or lossy dielectrics [4]. Despite this, these techniques are highly sensitive to surface properties of metals for detection of tight surface-breaking cracks, pitting and surface roughness evaluation [1,8–11].

There are a number of significant and practical advantageous features associated with these techniques, namely being non-contact, requiring low operating power, producing data in real time, being compatible with robotic systems for autonomous operation, producing high-resolution images of structures and being relatively inexpensive testing systems [1,2,12–14]. Consequently, there are many different microwave and millimetre-wave NDT&E techniques that have been developed for a diverse array of applications. This article provides a review of the technical foundations and applications of four specific microwave and millimetre-wave NDT&E techniques, namely materials characterization, surface crack detection, imaging and sensors. Given the limited space available in this article and in lieu of describing the technical and practical nuances of each method, a large number of references are provided for the interested reader.

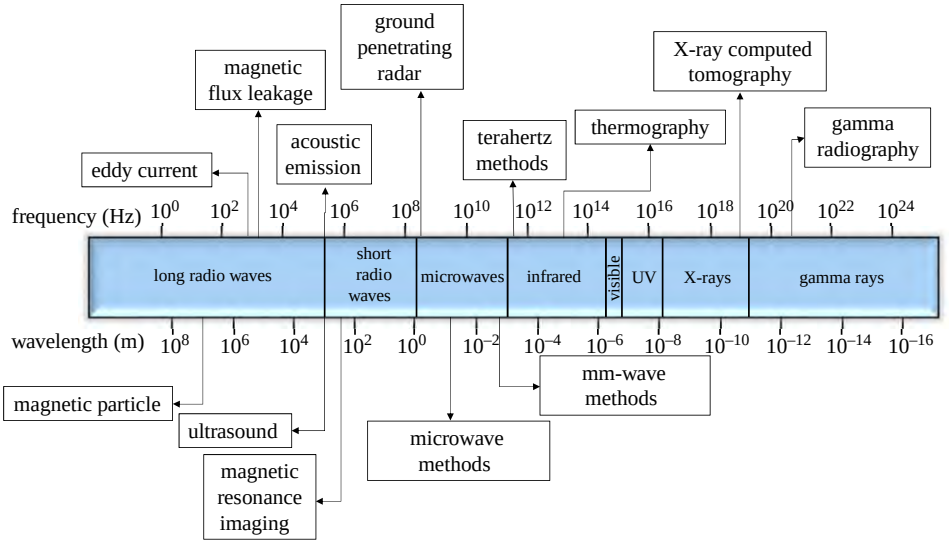


**Figure 1.** NDT&E techniques on the electromagnetic spectrum. (Online version in colour.)

## 2. Material characterization

Material characterization is at the heart of microwave and millimetre-wave NDT&E, since material properties can be correlated to the chemical and physical makeup, as well as the mechanical properties, of materials [1,4–6]. In addition, changes in material properties can be detected [1]. These in turn give insight into the 'state of the material' or MUT. At microwave frequencies, a material is intrinsically described by its complex permittivity, which is also called the complex dielectric constant. The complex permittivity, relative to free-space, denoted by $\varepsilon_r$, is comprises a real part or permittivity ($\varepsilon_r'$) and an imaginary part or loss factor ($\varepsilon_r''$), as $\varepsilon_r = \varepsilon_r' - j\varepsilon_r''$. The magnetic properties of a material are described by the relative permeability of a material, which is denoted as $\mu_r$ [5,15].

Permittivity indicates the propensity of a material to store microwave energy while loss factor indicates the tendency of a material to absorb microwave energy. Loss tangent is the ratio of the loss factor to permittivity. In general, permittivity tends to decrease with increasing frequency while loss tangent tends to increase with increasing frequency [4–7]. This becomes more of a complex relationship for mixtures made of a host and inclusions. Therefore, dielectric characterization of materials, over a wide frequency range, can provide valuable information about material properties. For a mixture, its 'effective' complex permittivity is directly dependent on the complex permittivities of the host and inclusions, their volume contents, any ongoing chemical reactions and the size of inclusions with respect to the operating wavelength (i.e. scattering and polarization). Dielectric mixing formulae can then be developed to predict the effective complex permittivity of mixtures and to back-calculate the individual contributions to the effective complex permittivity [5,6,16,17].

There are many methods for measuring complex permittivity over a wide range of frequencies. These methods can be broadly categorized as resonant, transmission/reflection and imaging techniques [7,18–21]. Additionally, the effects of other parameters such as sample preparation (for both destructive and non-destructive methods), sample surface roughness, moisture and temperature on the measurement results need to be considered when selecting a measurement method [7,16,17,22]. When using any of these methods, typically impedance, scattering parameters (S-parameters) or resonance frequency and quality (Q)-factor are measured [20].

Microwave and millimetre-wave materials characterization can therefore address a wide variety of NDT&E needs in applications such as cure-state monitoring in materials like

resins and rubber, determining critical materials properties in cementitious materials (e.g. water-to-cement, sand-to-cement and aggregate-to-cement), controlling mixture properties and determining porosity and distributed micro-cracking levels in materials like ceramics, thermal barrier coatings and plastics, to name just a few [7,12,23,24]. Application of specific sensors, such as patch antennas and chipless RFID tags, for materials characterization will be discussed separately in §5 along with other microwave and millimetre-wave sensors used for NDT&E.

## (a) Resonant techniques

Within the category of resonant techniques for materials characterization, there are a variety of different measurement systems that can be employed. For all of these, the general principle is to determine the resonance frequency and Q-factor and relate these parameters to the complex permittivities of the MUT. Some of these measurement systems are described below.

— Resonant and re-entrant cavity: capable of evaluating low loss materials with a high degree of accuracy at discrete frequencies, but requires that the sample be precisely machined and sample placement in the cavity is extremely critical. This renders the method (generally) destructive unless liquids or granular materials are being evaluated [22,25–34].
— Split-cylinder resonator: consists of a cylindrical cavity split into two sections. Laminar MUTs can be placed between the two sections to perform non-destructive materials characterization [7,35–37].
— Microstrip resonator: a resonator is fabricated on a substrate and the MUT is placed on top of the resonator to 'load' it. This changes the resonance characteristics and these changes are used to determine dielectric properties [38–40].
— Dielectric resonator: comes in many different form factors and has been used to characterize liquids, powders and thin films [41–44]. Split-post dielectric resonators are an offshoot of dielectric resonators that have been used to monitor the cure state of structural adhesive and to determine the dielectric properties of laminar samples over a wide range of temperatures [45–50].
— Open resonator: consists of two reflectors with a sample platform for solid laminar samples. They offer a non-contact solution and also have the advantages compared to cavity methods of being more broadband, having less stringent sample preparation requirements, and being able to more readily be used at millimetre-wave frequencies. They are also capable of studying anisotropic materials [51–56].

Employing all of these techniques implies that an electromagnetic (forward) model is available to describe the interaction of each specific system with material media. Subsequently, through an inverse model or a forward-iterative formulation, complex dielectric properties can be calculated [57,58].

## (b) Transmission and reflection techniques

Transmission media such as waveguides, coaxial cables, microstrip structures, co-planar waveguides and free-space systems can also be used for non-destructive materials characterization. This category of characterization methods can be further broken down into reflection methods and transmission/reflection methods [19,59].

In the category of reflection-based methods, primarily open-ended coaxial probes and open-ended waveguide probes are used. While these two techniques have similar implementations, they operate under different electromagnetic principles and provide different advantages and limitations. In both cases, the probe is placed against the surface of the MUT, or with a standoff between the probe and the MUT [60,61]. In relating the dielectric properties of the MUT to the response of the probe for both coaxial and waveguide probes, one can examine both the forward

method and the inverse method. In the forward method, the dielectric properties of the MUT are known and are used to determine the EM fields or response (e.g. $S_{11}$). In the inverse problem, the fields or response are known and are used with an iterative or optimization approach to determine the dielectric properties [62–67]. Errors can be introduced into the determination of dielectric properties by air gaps between the probe and the MUT, calibration errors and cable instability [1,19,61,68].

In comparing coaxial and waveguide open-ended probes, both have the advantage of being inherently broadband. However, waveguide probes can be used at higher frequencies than coaxial probes due to small (i.e. very high-frequency) coaxial probes being poor radiators which limits the signal penetration into the MUT [3,69,70]. For coaxial probes, sample (electrical) thickness plays a role in the accuracy of the characterization due to limited penetration depth, which is also related to the operating frequency and the flange size [1,19,61,64,66,71,72]. Owing to the way coaxial probes operate, they are well suited for characterizing liquids and malleable (soft) materials, like biological tissues [73,74]. Additionally, they can be used for characterizing thin multilayer structures, granular and aerated substances, and measuring salinity [1,65,66,75,76]. Open-ended waveguide probes operate similarly to coaxial probes except that instead of supporting transverse electromagnetic (TEM) wave propagation, they support transverse electric (TE) and transverse magnetic (TM) mode propagation and allow for inspecting electrically thick and multi-layered materials [1,19,57,77–85]. In principle, both coaxial and waveguide probes are capable of fully characterizing multilayer structures (i.e. algorithms can be used to solve for the complex permittivity and thickness of each layer), but in practice this is done more frequently with waveguides, primarily since penetration through several layers of reasonable thickness becomes a limiting factor for coaxial probes when evaluating multi-layered structures [61,65,77,82,86–88]. In addition, calibration of an open-ended waveguide probe is much more straightforward than that for a coaxial probe [61].

The development of the process to relate S-parameters to dielectric properties with a full-wave model for open-ended waveguide probes began in the 1980s [77,79–83,89,90]. From there higher order modes were added to the formulation and then the ability to determine the dielectric properties and thicknesses of each layer of a multilayer structure was achieved [57,86]. This has also been extended for examining gradient changes in dielectric properties which has applications in examining chloride permeation in concrete [91–95]. In both the forward and inverse models, an infinite flange is assumed. In order to match experiment with theory, a flange that appeared infinite while being physically realizable was needed and therefore developed [3,96,97]. In general, the open-ended waveguide technique is well suited for characterizing solid samples. Malleable materials and liquids can be characterized with this method [98–100]. However, care has to be taken so that the material does not protrude into the waveguide aperture, which can cause characterization inaccuracies [64]. Coplanar waveguides, while typically used in a transmission/reflection configuration, have also been used in a reflection configuration for characterizing these non-solid/stiff materials [101].

As previously mentioned, dielectric properties can be related to the chemical and physical makeup and mechanical properties of that material. The case discussed in [102] illustrates this and shows the utility of materials characterization for NDT&E. In this case, cement samples containing (reactive aggregate) and not containing (non-reactive aggregate) alkali–silica reaction (ASR) gel were temporally characterized using the open-ended waveguide method, and then an empirical dielectric mixing model was developed to examine the volume fractions (figure 2) and effective complex permittivities over time. By being able to monitor ASR gel formation in cement structures over time, valuable insight into the integrity of the MUT over its can be gained [102].

In the category of transmission/reflection methods, there are filled waveguide and coaxial methods, co-planar waveguide methods, microstrip methods and free-space methods. In these two-port methods, both $S_{21}$ and $S_{11}$ (transmission and reflection coefficient, respectively) measurements are used to determine the dielectric properties of a MUT [18–20,26,59]. A general

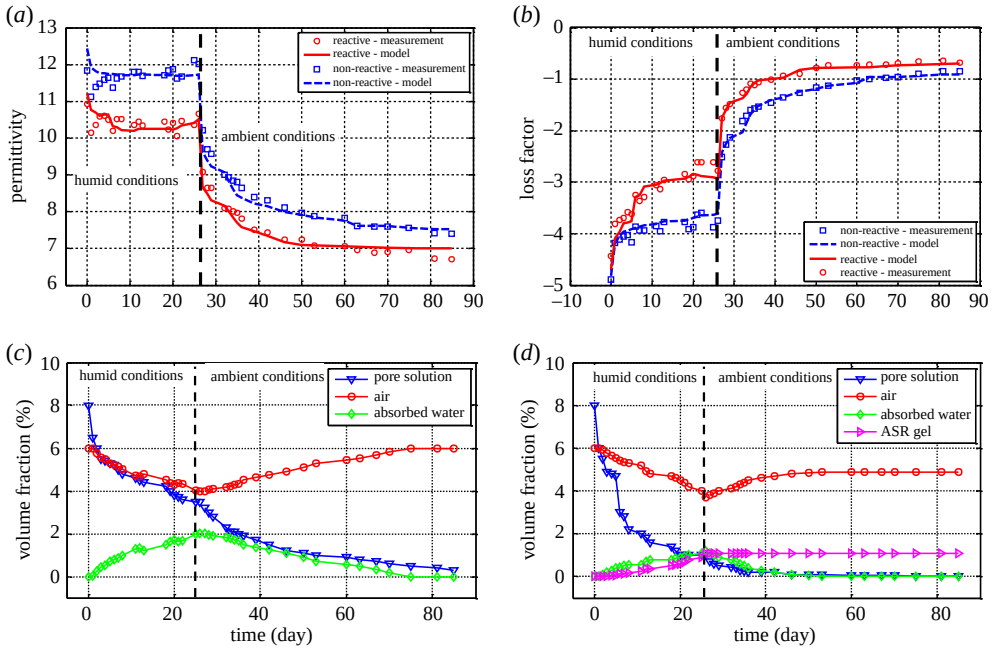


**Figure 2.** (*a*) Permittivity of ASR-reactive and non-reactive samples, (*b*) Loss factor of ASR-reactive and non-reactive samples, (*c*) Volume fractions of inclusions in non-reactive samples, and (*d*) Volume fractions of inclusions in reactive samples (©IEEE, 2017. Reprinted, with permission, from [102]). (Online version in colour.)

practical limitation of these techniques, especially for the free-space technique, is that for characterizing materials in structures it is not always possible to place measurement devices on both sides of the MUT. Another limitation is that for coaxial and waveguide methods the samples need to be precisely machined to fit within the transmission line without any gaps, meaning that these methods are destructive except when used to characterize liquids or granular materials [19,22]. These transmission techniques can be summarized as follows.

— Coaxial transmission line: barriers are used to hold a liquid or granular material in a portion of coaxial cable between the two measurement ports. Owing to penetration depth concerns, the length of coaxial line and the barriers need to be precisely chosen or calibration needs to be done up to the MUT to remove the influence of the barriers [3,69,103–105].
— Waveguide: a plug loaded method where dielectric plugs are used to hold the MUT in place during characterization has been developed. This allows for the multiple layers between the two measurement ports to be characterized [25,106].
— Coplanar waveguide: have the advantage of being very broadband and they have been used to characterize both solids and liquids. In the case of measuring liquids, coplanar waveguide devices can use smaller sample volumes than coaxial probes, which is advantageous for many biological applications [107–109]. Microstrip and stripline structures have been used similarly [7,110,111].
— Free-space: non-contact technique, which also makes it possible to use this technique to measure dielectric properties in high-temperature environments [19,112,113]. Traditional set-ups for this technique have a solid laminar sample placed between two horn antennas, but granular materials have also been used with sample holders with this technique [112,114–116].

### (c) Imaging/scanning

The last category of non-destructive materials characterization techniques are imaging-based techniques, which often involve scanning the MUT. Near-field probes, like the systems in the resonant devices section, use changes in resonance characteristics to determine dielectric properties and are often used in microwave microscopy systems. Owing to their resonant nature, these systems provide characterization at discrete frequencies. To determine the broadband dielectric properties curve fitting methods can be used. In these systems, the probe is scanned over an MUT and dielectric properties are determined at different locations. This information can then be formulated into an image [115,117–125].

A similar, yet different approach, is employing microwave imaging with synthetic aperture radar (SAR) processing to extract dielectric properties. This approach, which is very recent, uses a waveguide or horn antenna as the transducer rather than a near-field probe, meaning that this method is inherently more broadband than the near-field resonant probes used in microwave microscopy. While the method discussed in [126] provides only one complex permittivity value for the MUT, the method proposed in [21,127] can provide a distribution of dielectric properties for the MUT. In general, this technique shows great potential for spatially mapping dielectric properties in MUTs in a non-contact non-destructive manner. More information on microwave imaging and microwave microscopy are provided in §4.

As has been shown, there are many different microwave and millimetre-wave NDT&E techniques that can be used for materials characterization. While using imaging to generate spatial maps of dielectric properties of MUTs is the newest materials characterization technique, other recent developments and improvement areas of interest include creating measurement systems that are more compact, accurate and user-friendly; enhancing the speed of the algorithms used to determine dielectric properties; and better understanding the effects of other material properties and the environment on dielectric properties [31,116,127–132].

## 3. Surface crack detection

Although there exists a multitude of ‘standard’ NDT&E techniques for surface crack detection in metals, introduction of microwave and millimetre-wave techniques for this purpose dates back to the late 1960s [8–10,23]. However, in the past 25+ years, much has taken place with respect to the development and advancement of microwave and millimetre-wave techniques for detecting tight (fatigue) surface-breaking cracks in metals [1,2,11,23]. Although high-frequency signals do not penetrate conductive media such as metals, they can effectively interact with their surface properties. When a microwave or millimetre-wave signal irradiates a metal surface, it induces a surface current density [133,134]. Any type of surface anomaly, such as a surface-breaking crack, perturbs this current density, which in turn scatters some of the wave. The properties of the scattered wave depend on the frequency, probe characteristics, wave polarization, crack dimensions, whether the crack is filled with a dielectric (i.e. paint, rust) or covered with a coating of paint (and rust), etc. Therefore, a clear understanding of these electromagnetic properties can provide a significant amount of information about the ‘state’ of a crack [134–148]. The advantageous features of these techniques include, non-contact measurement, crack sizing capabilities, probe optimization for improved crack detection, detection of cracks under coatings and filled cracks, distinction between cracks and surface scratches and pitting, crack (preferred) orientation evaluation, rapid measurements, electromagnetic modelling capabilities leading to size evaluation and optimization and no signal clutter from within a conductive material.

Generally, microwave and millimetre-wave crack detection techniques involve scanning a probe over the MUT surface. Near-field techniques can be performed through one-dimensional (1D) or two-dimensional (2D) raster scans. Although crack detection is possible through far-field SAR techniques, near-field techniques have proven to be more effective when identifying small or tight cracks [149]. Thus, most of the techniques explored have been near-field techniques that use

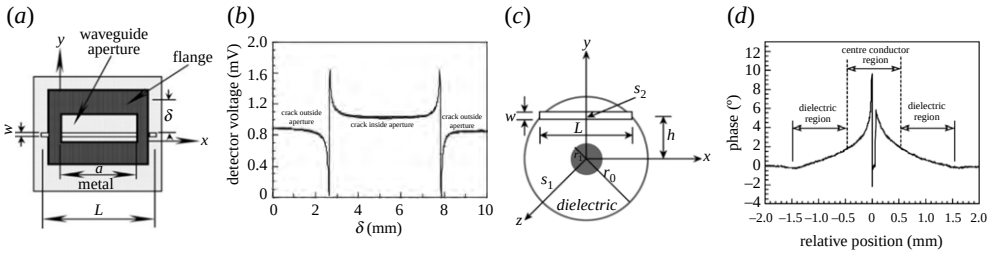


**Figure 3.** (*a*) Top view diagram of a surface crack and an open-ended rectangular waveguide and (*b*) measured voltage (proportional to reflection coefficient phase shift) versus probe location as it scans over the crack (© 1994 IEEE. Reprinted, with permission, from [131]). (*c*) Top view diagram of an open-ended coaxial probe scanning over a surface crack in a metal plate and (*d*) graph of the phase of the measured reflection coefficient as the probe moves over the crack (from [155] Copyright © 2002 by the American Society for Non-destructive Testing Inc. Reprinted with permission). (Online version in colour.)

open-ended rectangular waveguides [133,135–148,150–152], open-ended coaxial probes [153–158] and resonant probes [159–163], among others.

## (a) Open-ended waveguide probe

The use of microwave and millimetre-wave techniques for crack detection primarily depends on the interaction of a surface-breaking crack with induced surface current density on the metal surface. When using open-ended waveguides (the most widely applied probe), this surface current is generated through the excitation of the dominant TE mode of a rectangular waveguide, in which the electric field polarization vector points along the narrow dimension of the waveguide. When the waveguide aperture is placed near a metal surface, a surface current is induced on the metal surface which flows in the same direction as the electric field polarization vector. The presence of a surface-breaking crack near the waveguide opening, like in figure 3*a*, causes a perturbation in the induced surface current and consequently a shift in the phase of the reflection coefficient. This perturbation is maximal when the preferred crack length is perpendicular to the flow of the induced surface current, and thus the probe must be properly oriented relative to the crack.

The probe can be scanned over the metal surface while measuring the reflection coefficient seen by the waveguide. Figure 3*b* shows the measured voltage versus probe location (henceforth referred to as crack characteristic signal) for a long crack (crack length greater than the waveguide broad dimension) with width of 0.84 mm and a depth of 1.03 mm, measured with a K-band (18–26.5 GHz) waveguide at 24 GHz. This measured voltage is proportional to the shift in phase of the reflection coefficient seen by the probe [133].

In-depth modelling of this crack characteristic signal has allowed for better detection capabilities and more optimal probe design [144] and additionally has given way to methods of crack sizing through the matching of the crack characteristic signal to the model, most notably width and depth determination [137,143]. Determining the crack length, or rather the locations of the crack tips, can be performed by identifying the crack tip characteristic signal while scanning along the preferred crack length [138]. Other crack sizing techniques that have been explored include, depth determination using resonant frequency measurements [147,148] and the consideration of higher order modes generated by the presence of a crack to better facilitate detection [135]. Open-ended waveguide techniques have also been used in differential probe-based systems, consisting of two waveguides situated side-by-side, where the output of the system is the difference in reflection coefficient seen by the two waveguides. This configuration allows the effect of perturbations located in only one waveguide, such as a crack, to be isolated, thereby eliminating the effect of common signals, such that those caused by covering paint layers

and non-uniform surfaces [145,164]. This methodology has also been applied for crack detection in concrete structures [165].

### (b) Other probes

The effectiveness of the open-ended waveguide probe gives rise to alternative probe types relying on the same operational principle. Most notable are open-ended coaxial probes, shown in figure 3*c*, which have a couple primary advantages over rectangular waveguide probes. One advantage arises from the dominant TEM mode of the coaxial probe, which is inherently wideband. This large bandwidth gives a high degree of flexibility in regards to probe size, allowing cracks to be detected that are thousands of times narrower than the operating wavelength. Another significant advantage of this type of probe is its radial symmetry and thus its lack of a preferred electric field polarization vector direction, which eliminates crack orientation as a concern. The advantages it provides have made the open-ended coaxial probe a viable tool for crack detection [153–155,157].

The graph in figure 3*d* shows the phase of the measured reflection coefficient as the coaxial probe moves over the crack in a direction perpendicular to the crack preferred length for a long crack with width of 0.152 mm and a depth of 1 mm, using a coaxial probe inner and outer radius 0.5 mm and 1.5 mm, respectively, at 10 GHz [156,157]. This crack characteristic signal illustrates the high sensitivity of the coaxial probe to crack dimensions, even at a relatively low frequency (the wavelength at 10 GHz is 30 mm and the crack indication width is less than 0.2 mm). Although this sensitivity gives way to methods of crack sizing, it can also be a disadvantage, since even tiny perturbations in the probe geometry can have a large effect on the crack characteristic signal, leading to discrepancies between the model and measurements. Much work has gone into modelling of the interactions of this type of probe with surface-breaking cracks [156–158,166]. Recently, improvements in the modelling of the open-ended coaxial probe includes the consideration of a cone shaped aperture profile, resulting in a better understanding of the critical geometries in the probe design [158].

Other crack detection techniques make use of resonant frequency shifts to indicate cracks. This type of crack detection sensor generally consists of an electromagnetic resonator combined with an interrogating probe capable of exciting the resonator and measuring its resonant frequency. When a resonator is scanned over a metal surface, a surface-breaking crack interacts with the electric field, consequently initiating a measurable shift in resonant frequency. The resonant frequency can then be measured as a function of probe location, where a large shift in frequency indicates a nearby crack. The split-ring resonator design has been proven to be effective for crack detection [159–163] and has been successfully demonstrated using microstrip lines [159–161], waveguides [162] and substrate-integrated waveguides [163] as interrogating probes. Resonant frequency-based crack detection techniques have also shown some promise in crack sizing, exploiting the relationship between crack dimensions and the amount of resonant frequency shift [162].

As shown here, there are a variety of microwave and millimetre-wave NDT&E techniques that can be used in crack detection applications. Additionally, there is a large potential for the utility of polarimetric measurements (i.e. dual-polarized probes, circular polarization, etc.) for crack detection and characterization. Future research will explore this potential and will include further development and expansion of the efficacy of far-field (SAR-based) techniques for rapid detection, sizing and characterization of surface-breaking cracks in metals, as well as improvements upon existing near-field techniques.

## 4. Imaging

Microwave and millimetre-wave imaging is the process of creating a 2D (or three-dimensional (3D)) map of electromagnetic properties of a MUT [1]. The electromagnetic property can be an intrinsic material property, such as relative complex permittivity ($\varepsilon_r$) or relative permeability ($\mu_r$),

or can be quantities that are proportional to these material properties such as reflectivity as well as geometrical features (e.g. a crack) [1,167]. Therefore, such images are produced as a function of material property contrast in an object and geometry (relative to the operating wavelength). Microwave imaging probes are essentially antennas. Hence, imaging techniques can primarily be classified as either near-field or far-field techniques depending on the (electrical) distance between the probe and the MUT [15,168]. Microwave images are primarily produced using raster scanning, although in lieu of mechanical (raster) scanning, 1D and 2D arrays of antennas can be assembled, to perform rapid electronic scanning. In either case, a 2D matrix consisting of measured data, commonly a DC voltage or complex scattering parameters, as a function of frequency and proportional to the local reflection properties in a specimen is obtained [168]. The collected data are then mapped directly to a contrast image or processed using backpropagation algorithms (e.g. SAR) [167–169]. Thus, the choice of imaging technique, probe type and frequency of operation are dependent on the sample properties and the target features (e.g. crack, void, delaminations, etc.).

## (a) Near-field imaging and microwave microscopy

Near-field microwave imaging is performed with a relatively small (electrical) distance between the probe and the surface of the MUT. In the near-field region, the high sensitivity due to the presence of reactive evanescent waves, as well as high-resolution imaging due the concentrated electromagnetic energy (i.e. small-sized probes), are possible. The image resolution in near-field scanning is mainly governed by the physical aperture size of the probe (i.e. not diffraction limited) producing very high-resolution ($< \lambda/100$ or better) images using relatively simple probes with very small (compared to wavelength) apertures [1,170]. Near-field image resolution and sensitivity to sample variations and flaws are functions of probe aperture size, electromagnetic field distribution in the near-field of the probe and distance to MUT (i.e. standoff distance). Near-field electromagnetic field distribution is a strong function of distance away from a probe, which makes near-field imaging very sensitive to standoff distance and more importantly to its variation during a scan [144,171]. There are several different types of near-field probes that may be used (open-ended rectangular and circular waveguides, open-ended coaxial lines, microstrip patches, cavity resonators, etc.), each providing its own unique advantageous features and limitations for a specific application [1]. Open-ended rectangular waveguide antennas are widely used for near-field imaging due to ease of integration with microwave and millimetre-wave circuits, availability of standard waveguide calibration kits, and for being a reasonably efficient antenna over the complete waveguide band. Furthermore, the dimensions of the waveguide aperture are on the order of $\lambda/2$ and $\lambda/4$ on each side providing images resolutions matching or higher than the diffraction limit without any post-processing. The open-ended waveguide probe aperture geometry can be further modified (reduced in size) to increase resolution and sensitivity to flaws. An example of these modifications is tapering the waveguide to a smaller aperture and using a thin dielectric slab as an insert which focuses the electric field [144,148]. For microwave microscopy, probes have been designed that incorporate very small probe tip, along with a resonator to achieve super-resolution. Microwave microscopy techniques provide limited penetration depth; however, they can be used to characterize surface properties of metals, semiconductors and dielectrics with great accuracy, provided extreme consistency in standoff distance during testing [170].

As described earlier, maximum sensitivity to sample variations can be obtained at the near-field of the probe. Yet at those distances, the probe is also very sensitive to variations in the standoff distance which can be caused by misalignments between the scanning platform and the MUT surface or by sample surface curvature. This high sensitivity to standoff distance variation can prove detrimental when the target defects are small or low-scattering such as tight and short cracks and surface micro-pitting in metals [146]. Several techniques have been proposed that perform compensation for standoff distance variation, such as a potentiometer in contact with

the sample [171], using a dual aperture differential probe [146], and a dual-polarized probe which is used on polarized surfaces like unidirectional carbon fibre composite [172].

## (b) Far-field imaging with focusing lenses

In near-field imaging, resolution and sensitivity degrade rapidly with distance since the radiated electric field from a small probe expands rapidly with distance. In some applications, such as when imaging thick composite structures (depending on the material properties), operation from a larger distance (far-field) becomes necessary. Therefore, to maintain image resolution and sensitivity from this distance an antenna with a focused beam may be used. A lens antenna provides a focused electric field pattern and subsequently high resolution at a distance corresponding to its focal length. Lens focusing is practical, for NDE applications, at single frequencies in the millimetre-wave frequency range on the order of 50 GHz or higher due to required electrically large aperture lens. A drawback of using lens antennas is that their focal point is only at a specific distance from the antenna and also changes with frequency. Furthermore, this focal point is typically specified for operation in air; therefore, the focusing capabilities of the antenna can further degrade when used to image materials with a relatively high permittivity and loss. High-resolution imaging using lens antennas has been successfully demonstrated for imaging through thick spray on foam insulation samples for the detection of voids and delamination [173].

## (c) Synthetic aperture radar imaging

Microwave and millimetre-wave imaging using antennas or lenses for focusing microwave or millimetre-wave signals are referred to as 'real-aperture' focused techniques. Practical real apertures reported in the literature are relatively large antennas with a diameter up to 100λ which provide an aperture-limited resolution on the order of approximately 2–5λ. Additionally, such real-aperture techniques are only focused at one plane at its focal distance as mentioned above [173]. High-resolution imaging methods, based on (backpropagation) SAR algorithms, are capable of producing 3D holographic images of dielectric structures. Such imaging methods are extremely valuable for inspecting the ever-increasingly used nonconductive composite structures that have been replacing metals in many industries [174,175]. Figure 4*a* shows the fundamental principle of SAR imaging. A small antenna (with broad radiation pattern) is raster scanned along a 1D path or across a 2D grid forming a synthetic array or aperture [176]. The antenna is connected to a wideband reflectometer which performs coherent (referenced) reflection measurements from multiple angles (views) of the sample. The collected reflected data is then processed by a fast 3D SAR algorithm (e.g. ω-k algorithm) to produce a 2D or 3D holographic image of the sample under test. Figure 4*b* shows a comparison between an X-ray and a millimetre-wave (Ka-band, 26.5–40 GHz) SAR image of an adhesive joint in a fibreglass structure. Similar to X-ray, the SAR image shows the locations of the missing adhesive while also showing higher sensitivity to the non-uniformity of the fibreglass structure. SAR imaging provide range (depth) resolution:

$$\delta_z = \frac{v}{2B}. \tag{4.1}$$

In equation (4.1), $v$ is the wave velocity inside the material and $B$ is the bandwidth of the microwave signal. The cross-range resolution is on the order of $\lambda/4$ at distance close to the synthetic array and it degrades (becomes aperture limited) as distance increases [169].

Many composite structures are made of multiple stratified layers of dielectric materials, each with a permittivity value. Additionally, often there is a layer of air (i.e. standoff distance) between the synthetic aperture and the surface of the sample. SAR algorithms can be made to account for the permittivities of these various layers to properly compensate for the coherent wave propagation through these multi-layered materials. Recently, two SAR-based techniques were developed for microwave imaging of embedded objects inside of layered structures. The first method, piecewise SAR (PW-SAR), which considers physical/electrical properties of each layer

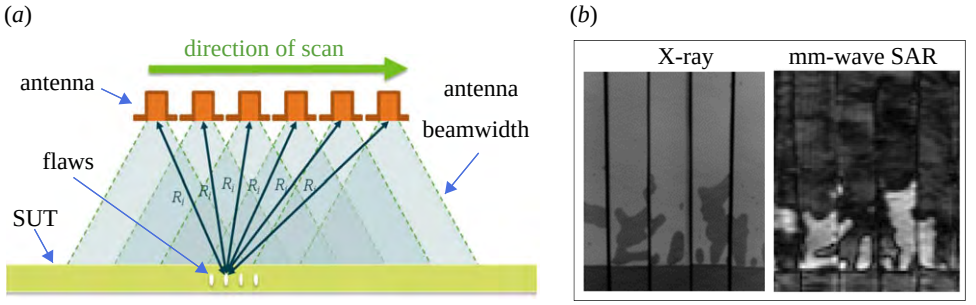


**Figure 4.** (*a*) Schematic of synthetic aperture imaging using a small antenna and (*b*) a comparison between an X-ray and a millimetre-wave (26.5–40 GHz) image of voids in an adhesive joint of a fibreglass structure. (Sample and X-ray image are courtesy of Fibreglass Structural Engineering). (Online version in colour.)

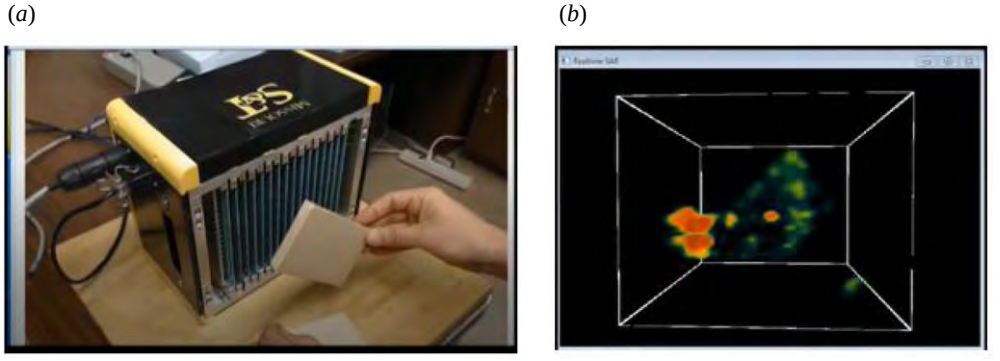


**Figure 5.** (*a*) Picture of microwave camera scanning a wood composite with an imbedded rubber insert and (*b*) a screen capture of the produced real-time 3D image of the wood composite, also showing the operator's fingers. (Online version in colour.)

between the scanning antenna and the object. The second method is rather comprehensive, namely, a Wiener filter-based layered SAR (WL-SAR) which relies on the Green function model of layered structures [177]. Calibrated SAR images can also be used to generate high-resolution quantitative images showing the complex permittivity in a material [21]. A 3D imaging can also be performed in non-Cartesian planes (e.g. cylindrical) using the appropriate algorithms such as SAR or time reversal [167,178,179].

A major benefit of SAR imaging is that it can be performed using physical antenna arrays which enables production of real-time images [176,180–182]. Early imaging array designs used modulated scattering techniques [176,180]. SAR imaging can also be performed using simple interferometric reflectometers. The major advantage of such a reflectometer is that its output is phase-referenced to the aperture of the imaging probe (e.g. an open-ended waveguide) for all frequencies, thus no post-measurement phase-referencing (i.e. calibration) is required for wideband operations [183]. Such a design allows for building compact and relatively low-cost, real-time, portable and wideband (3D) imaging arrays (or a microwave camera) [184–186]. Figure 5 shows a picture of a microwave camera that is capable of producing images at a frame rate of up to 30 frames per second and a screen capture of a 3D image produced in real time of a wood composite sample with an embedded rubber piece in its centre [184]. With the rapid and continual advancement in millimetre-wave integrated circuits, designs of microwave and millimetre-wave imaging systems are constantly evolving and optimized more-capable designs for specific applications are becoming possible.

## 5. Sensors and sensing

In the area of microwave and millimetre-wave NDT&E, sensors have been developed to monitor a wide variety of measurands including temperature, strain, dielectric properties, torque, humidity and much more. Broadly, these sensors can be categorized as either wireless or wired and as either active or passive. Furthermore, they can be described by whether they operate in the time or frequency domain, by whether they provide distributed or localized sensing capabilities, and by how they interact with material or structure they are monitoring [187,188]. Given the breadth of the area of sensing for NDT&E, only three categories and microwave and millimetre-wave sensing solution are discussed in the context of two examples each: sensing with transmission media probes, wired solutions and wireless passive solutions.

### (a) Sensing with transmission media probes

In previous sections, both waveguides and coaxial cables were discussed in the context of multiple applications. Additionally, these probes have been used for other NDT&E sensing purposes. Coaxial cables have been used to create sensors for nanometre scale displacement sensing and crack/strain sensing in reinforced concrete, to name just two of many examples [189,190]. In using coaxial cables as sensors, optical devices, like Fabry–Perot interferometers and Bragg gratings, have been used as inspiration [189,191–196]. In the case of the displacement sensor, an open-ended hollow coaxial cable resonator was created with its resonance characteristics being sensitive to changes in displacement. While inspired by optical devices, this sensor is much more rugged than optical fibre-based sensors, while also being less expensive and operating in the microwave frequency regime [189]. Another coaxial sensing technique uses changes in the outer conductor with time domain reflectometry (TDR) to provide distributed sensing of cracks and strain. This solution in comparison to the previous displacement sensor example would be embedded in a structure making it more invasive [190].

Beyond being able to be used for materials characterization, crack detection and imaging, waveguides have additional sensing applications including thickness determination, disbond and corrosion detection, to provide a few examples [1,23,60]. When using waveguides, thickness determination and detecting disbonds can go hand in hand. These two NDT&E applications are typically done for layered composite materials that are either backed by free-space, dielectric layers or a conductor [1,23]. The disbonds appear as air gaps between the layers and the thickness of the disbond as well as the thickness of the layers can be determined. This is done by relating how the magnitude and phase of an $S_{11}$ measurement from an open-ended waveguide change due to thickness through models and algorithms [60,197,198]. As previously discussed in §2, thickness can also be determined for multiple layers while performing materials characterization [86].

### (b) Wired solutions

Wired solutions tend to be more invasive than wireless or probe-based solutions. Modulated scatter technique (MST) probes and microstrip patch antennas are two types of typically wired microwave and millimetre-wave sensors that have been used for NDT&E applications. MST probes are typically small dipole antennas loaded with lumped elements (e.g. PIN diodes) that are modulated by an external source. By modulating the probe, the wave it scatters is also modulated making it easier to distinguish from background reflections. MST probes have found applications in NDT&E by being used as sensors for dielectric properties, corrosion and disbonds [199–205]. By being embedded into structures, they can be used to sense local structural integrity and perform monitoring over time [199,206–209]. While these sensors haven't come into practical use, they have laid the foundation for other embedded microwave sensors [210].

Microstrip patch antennas have also been used as sensors by either being embedded or attached to materials or structures [187,211]. As with the previously discussed types of

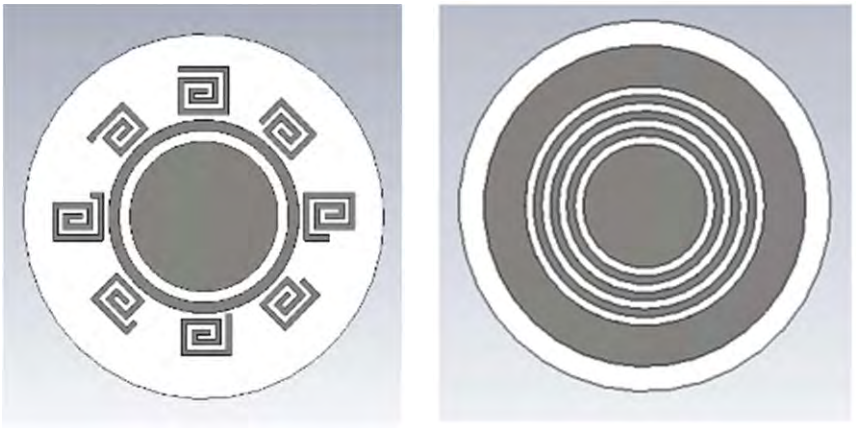

**Figure 6.** Chipless RFID tag examples. (Online version in colour.)

sensors, this type of sensor has also been used for many different applications, including temperature [212,213], strain [214–217], dielectric properties [212,218,219] and crack sensing [220]. Being planar, patch antennas can also be made to be flexible and/or conformal to the structures they will monitor [214].

## (c) Wireless passive sensors

Wireless passive sensors contain no power source and no physical transmission media (i.e. cable) connection back to instrumentation. In the microwave and millimetre-wave regime, these sensors are interrogated with an electromagnetic wave and their response is correlated to sensing parameters. One type of these sensors are frequency selective surfaces (FSS), which are planar periodic arrays of conductive shapes or slots cut out of conductor planes that create a specific frequency response (typically resonant) to an interrogating electromagnetic wave [221,222]. While an FSS can be active or passive, passive FSSs are the focus here [223]. FSSs have been widely used in radome and filtering applications, but have also found a role in sensing-based NDT&E [221,222]. For FSS-based sensors, typically either a material that is sensitive to the sensing parameter (e.g. temperature sensitive dielectric) or a unit cell element that is sensitive to the sensing parameter (e.g. a cross loop whose resonance characteristics are sensitive to strain) are used [224–226]. These two sensing methods can also be combined to create an FSS that is capable of sensing multiple parameters simultaneously, which is especially useful in cases where one needs to understand the effect of one parameter on another like is the case with strain and temperature [227]. Beyond temperature and strain sensors, FSSs have also been used for crack detection and materials characterization [228–231].

Radio frequency identification (RFID) systems can also be used for NDT&E and consist of a reader and a tag. Chipless RFID is the newest area within the RFID field and is thus discussed here [232–234]. Chipless tags, having no power source and no IC, instead 'store' their information in their tag structure. Examples of tags are shown in figure 6. When interrogated with an EM wave, the tag's response (typically the radar cross-section (RCS) versus frequency or $S_{11}$ response) reveals this stored information [235,236]. A binary code can then be assigned to this response, which typically contains a collection of resonances. Manipulating the tag structure or the environment that the tag is in causes a change in this response and in turn changes the binary code. This mechanism is typically used to perform identification, but can also be used to perform sensing [235].

Chipless RFID sensor tags have been developed for sensing a wide variety of phenomena including temperature, corrosion, strain, rotation, displacement, humidity, cracks and dielectric

properties [210,237–253]. With these sensor tags, there are four common ways in which the response is translated into a sensing parameter

- Associating a resonance frequency shift with a sensing parameter [238,250].
- Associating a magnitude change in a peak or notch with a sensing parameter [244,254].
- Associating a response shape change with a sensing parameter [255].
- Associating a change in tag characteristics, such as gain or maximum RCS, with a sensing parameter [252,253,256].

As previously inferred, beyond these sensing mechanisms binary codes can also be assigned to responses and the change in the code can be used to perform sensing [210,235]. Owing to this technology still being relatively new with the first chipless tags being reported in 2007, there are still many challenges to overcome like tag localization, read range extension, tag detection, orientation sensitivity and manufacturing tags in a quick and inexpensive fashion so they can be widely deployed [235,257–260].

As can be seen, there are a wide variety of microwave and millimetre-wave sensors that can be used for NDT&E purposes. Owing to their minimally invasive nature and long lifetime, wireless passive sensors are of growing interest. In making this type of sensor more practical, there are a variety of advancements being made including lower power electronics [261,262], new energy harvesting circuits [263–265], using inkjet-printing for inexpensive fabrication [266,267], extending read ranges for non-contact long range monitoring [258,268–270], developing novel post-processing techniques [259,271,272] and creating more robust sensors for extreme environments [273,274], to name a few.

## 6. Conclusion

As has been shown, the field of microwave and millimetre-wave NDT&E has broad applicability; while these techniques are limited in terms of penetration capabilities of conductive materials, they are optimal for dielectric material inspection and can be used for examining surface-breaking defects of conductive materials. Techniques such as open-ended waveguide materials characterization, coaxial probe surface crack detection, microwave SAR imaging and embedded high-frequency sensors provide a broad range of inspection capabilities across many different application areas including, security, aerospace, biomedical and civil. It is expected that these methods will see more utility in the future, especially as high-frequency components become more readily available commercially and as form factors and costs reduce as a result. In addition, these techniques can be combined with other NDT&E techniques to enhance inspection capabilities [275,276]. Furthermore, as areas such as AI, IoT and image and signal processing advance, it is envisioned that they will be more widely applied to microwave and millimetre-wave NDT&E as they are in other NDT&E methods.

Data accessibility. This article has no additional data.

Authors' contributions. K.B. provided the materials characterization and sensing sections while also coordinating the authorship team. M.D. provided the surface crack detection section. M.T.A.Q. and R.Z. provided the imaging section. R.Z. and K.B. collaborated on the introduction and conclusion. All authors contributed to and approved the manuscript.

Competing interests. We declare we have no competing interests.

Funding. We received no funding for this study.

## References

1. Zoughi R. 2000 *Microwave Non-destructive testing and evaluation principles*. Dordrecht, The Netherlands: Springer.
2. Schull P, Dekker M. 2002 *Nondestructive evaluation: theory, techniques, and applications*, 1st edn. Boca Raton, FL: CRC Press.

3. Case JT, Kenderian S. 2017 Microwave NDT: an inspection method. *Mater. Eval.* **75**, 339–346.
4. Balanis CA. 1989 *Advanced engineering electromagnetics*. New York, NY: John Wiley and Sons.
5. Ulaby FT, Moore RK, Fung AK. 1986 *Microwave remote sensing, active and passive appendix E. III*. Dedham, MA: Artech House.
6. Sihvola A. 1999 *Electromagnetic mixing formulas and applications*. London, UK: IET Publishing.
7. Baker-Jarvis J, Janezic MD, Degroot DC. 2010 High-frequency dielectric measurements. *IEEE Instrum. Meas. Mag.* **13**, 24–31. (doi:10.1109/MIM.2010.5438334)
8. Feinstein L, Hruby RJ. 1967 *Surface crack detection by microwave methods*. San Antonio, TX: NASA.
9. Ash EA, Husain A, editors. 1973 Surface Examination using a Superresolution Scanning Microwave Microscope. In *3rd European Microwave Conference*, 4–7 Sept, 1973.
10. Auld BA. 1981 Ferromagnetic resonance flaw detection. *Phys. Technol.* **12**, 149–154. (doi:10.1088/0305-4624/12/4/I03)
11. Zoughi R, Kharkovsky S. 2008 Microwave and millimetre wave sensors for crack detection. *Fatigue Fract. Eng. Mater. Struct.* **31**, 695–713. (doi:10.1111/j.1460-2695.2008.01255.x)
12. Kharkovsky S, Zoughi R. 2007 Microwave and millimeter wave nondestructive testing and evaluation - Overview and recent advances. *IEEE Instrum. Meas. Mag.* **10**, 26–38. (doi:10.1109/MIM.2007.364985)
13. Carrigan TD, Forrest BE, Andem HN, Gui K, Johnson L, Hibbert JE, Lennox B, Sloan R. 2019 Nondestructive testing of nonmetallic pipelines using microwave reflectometry on an in-line inspection robot. *IEEE Trans. Instrum. Meas.* **68**, 586–594. (doi:10.1109/TIM.2018.2847780)
14. Abou-Khousa MA, Ryley A, Kharkovsky S, Zoughi R, Daniels D, Kreitinger N, Steffes G. (eds). 2006 Comparison of X-Ray, Millimeter Wave, Shearography and Through-Transmission Ultrasonic Methods for Inspection of Honeycomb Composites. In *Thrity-Third Annual Review of the Quantitative Nondestructive Evaluation Conf., 2007/03/21, Portland, Oregon*.
15. Balanis CA. 2012 *Antenna theory: analysis and design*. Hoboken, NJ: John Wiley & Sons.
16. Gregory A, Lees K, Clarke B, NPL. 2013 *Good practice in specimen preparation, specimen handling & thickness measurement*. Teddington, UK: National Physical Laboratory.
17. Kraszewski A. 1996 *Microwave aquametry*. New York, NY: IEEE Press.
18. You KY, Esa FB, Abbas Z (eds). 2017 Macroscopic characterization of materials using microwave measurement methods — A survey. In *Progress in Electromagnetics Research Symp. - Fall (PIERS - FALL), 19–22 Nov. 2017*.
19. Technologies K. 2019 Basics of measuring the dielectric properties of materials. See https://www.keysight.com/us/en/assets/7018-01284/application-notes/5989-2589.pdf.
20. Rohde&Schwarz. 2012 Measurement of dielectric material properties. See https://cdn.rohde-schwarz.com/pws/dl_downloads/dl_application/00aps_undefined/RAC-0607-0019_1_5E.pdf.
21. Gao Y, Ghasr MT, Zoughi R (eds). 2019 Spatial mapping of complex permittivity from synthetic aperture radar (SAR) images. In *IEEE International Instrumentation and Measurement Technology Conference (I2MTC)*, 20–23 May 2019.
22. Foudazi A, Donnell KM. 2016 Effect of sample preparation on microwave material characterization by loaded waveguide technique. *IEEE Trans. Instrum. Meas.* **65**, 1669–1677. (doi:10.1109/TIM.2016.2540840)
23. Bahr AJ. 1982 *Microwave nondestructive testing methods*. New York, NY: Gordon and Breach Science Publishers.
24. Hashemi A, Horst M, Kurtis KE, Donnell KM, Zoughi R. 2015 Comparison of alkali–silica reaction gel behavior in mortar at microwave frequencies. *IEEE Trans. Instrum. Meas.* **64**, 1907–1915. (doi:10.1109/TIM.2014.2367771)
25. Bois KJ, Handjojo LF, Benally AD, Mubarak K, Zoughi R. 1999 Dielectric plug-loaded two-port transmission line measurement technique for dielectric property characterization of granular and liquid materials. *IEEE Trans. Instrum. Meas.* **48**, 1141–1148. (doi:10.1109/19.816128)
26. Sheen J. 2009 Comparisons of microwave dielectric property measurements by transmission/reflection techniques and resonance techniques. *Meas. Sci. Technol.* **20**, 042001. (doi:10.1088/0957-0233/20/4/042001)
27. Sproull RL, Linder EG. 1946 Resonant-cavity measurements. *Proc. IRE.* **34**, 305–312. (doi:10.1109/JRPROC.1946.229636)

28. Roggen AV (ed.). 1970 Rapid dielectric permittivity measurements at microwave frequencies. In *Conf. on Electrical Insulation & Dielectric Phenomena – Annual Report*, 12–14 Oct, 1970.
29. Datta S, Vinoy KJ (eds). 2018 Design of a Compact Radio Frequency Cavity Resonator as a Sensor for Dielectric Liquids. In *IEEE MTT-S International Microwave and RF Conf. (IMaRC)*, 2018 28–30 Nov. 2018.
30. Alvarez JO, Peñaranda-Foix FL, Catalá-Civera JM, Gutiérrez-Cano JD. 2019 Permittivity spectrum of low-loss liquid and powder geomaterials using multipoint reentrant cavities. *IEEE Trans. Geosci. Remote Sens.* **58**, 1–16.
31. Kapilevich B, Litvak B, Balavin A. 2013 Microwave characterization of powders using multiresonance cell. *IEEE Trans. Instrum. Meas.* **62**, 408–414. (doi:10.1109/TIM.2012.2215140)
32. Marqués-Villarroya D, Pcñaranda-Foix F, Canós AJ, García-Baños B, Catalá-Civera JM (eds). 2018 Determination of the complex permittivity of high loss liquids with a novel reentrant cavity. In *IEEE/MTT-S International Microwave Symposium – IMS*, 10–15 June 2018.
33. Kams DC *et al.* (eds). 2018 Millimeter-wave resonant cavity for complex permittivity measurements of materials. In *IEEE/MTT-S International Microwave Symp. – IMS*, 10–15 June 2018.
34. Kawabata H, Tanpo H, Kobayashi Y (eds). 2003 A rigorous analysis of a TM/sub 010/ mode cylindrical cavity to measure accurate complex permittivity of liquid. In *33rd European Microwave Conf. Proc. (IEEE Cat No03EX723C)*, 7–7 Oct. 2003.
35. Janezic MD, Baker-Jarvis J. 1999 Full-wave analysis of a split-cylinder resonator for nondestructive permittivity measurements. *IEEE Trans. Microwave Theory Tech.* **47**, 2014–2020. (doi:10.1109/22.795077)
36. Kent G. 1996 Nondestructive permittivity measurement of substrates. *IEEE Trans. Instrum. Meas.* **45**, 102–106. (doi:10.1109/19.481319)
37. Marqués-Villarroya D, Peñaranda-Foix FL, García-Baños B, Catalá-Civera JM, Gutiérrez-Cano JD. 2017 Enhanced full-wave circuit analysis for modeling of a split cylinder resonator. *IEEE Trans. Microwave Theory Tech.* **65**, 1191–1202. (doi:10.1109/TMTT.2016.2637932)
38. Bernard PA, Gautray JM. 1991 Measurement of dielectric constant using a microstrip ring resonator. *IEEE Trans. Microwave Theory Tech.* **39**, 592–595. (doi:10.1109/22.75310)
39. Hardinata S, Deshours F, Alquié G, Kokabi H, Koskas F (eds). 2018 Complementary split-ring resonators for non-invasive characterization of biological tissues. In *18th Int. Symp. on Antenna Technology and Applied Electromagnetics (ANTEM)*, 19–22 Aug, 2018.
40. Rashidian A, Aligodarz MT, Klymyshyn DM. 2012 Dielectric characterization of materials using a modified microstrip ring resonator technique. *IEEE Trans. Dielectr. Electr. Insul.* **19**, 1392–1399. (doi:10.1109/TDEI.2012.6260016)
41. Tiwari NK, Sharma A, Singh SP, Akhtar MJ, Biswas A (eds). 2019 Non-invasive dielectric characterization of chemical solvents using microstrip-fed dielectric resonator based sensor. In *URSI Asia-Pacific Radio Science Conf. (AP-RASC), 9–15 March 2019*.
42. Bovtun V, Pashkov VV, Kempa M, Molchanov V, Kamba S, Poplavko Y, Yakymenko Y. (eds). 2011 Thin dielectric resonators for microwave characterization of films and substrates. In *21st Int. Crimean Conference 'Microwave & Telecommunication Technology'*, 12–16 Sept. 2011.
43. Hakki BW, Coleman PD. 1960 A dielectric resonator method of measuring inductive capacities in the millimeter range. *IRE Trans. Microw. Theory and Tech.* **8**, 402–410. (doi:10.1109/TMTT.1960.1124749)
44. Yasin A, Shafique MF, Amin S, Khan MA. 2019 Rapid characterization of powder mixtures through high Q dielectric resonator. *ECS J. Solid State Sci. Tech.* **8**, N13. (doi:10.1149/2.0081902jss)
45. Givot BL, Krupka J, Belete DY. (eds). 2000 Split post dielectric resonator technique for dielectric cure monitoring of structural adhesives. In *13th Int. Conf. on Microwaves, Radar and Wireless Communications MIKON – 2000 Conference Proceedings (IEEE Cat No00EX428)*, 22–24 May 2000.
46. Krupka J, Clarke RN, Rochard OC, Gregory AP (eds). 2000 Split post dielectric resonator technique for precise measurements of laminar dielectric specimens-measurement uncertainties. In *13th Int. Conf. on Microwaves, Radar and Wireless Communications MIKON – 2000 Conf. Proc. (IEEE Cat No00EX428)*, 22–24 May 2000.

47. Givot BL, Krupka J, Derzakowski K (eds). 2002 Split-post dielectric resonator for complex permittivity measurements at 20–25 GHz. In *14th Int. Conf. on Microwaves, Radar and Wireless Communications MIKON - 2002 Conf. Proc. (IEEE CatNo02EX562)*, 20–22 May 2002.
48. Mazierska J, Krupka J, Jacob MV, Ledenyov D (eds). 2004 Complex permittivity measurements at variable temperatures of low loss dielectric substrates employing split post and single post dielectric resonators. In *IEEE MTT-S Int. Microwave Symp. Digest (IEEE Cat No04CH37535)*, 6–11 June 2004.
49. Korpas P, Wojtasiak W, Krupka J, Gwarek W (eds). 2012 Inexpensive approach to dielectric measurements. In *19th International Con. on Microwaves, Radar & Wireless Communications*, 21–23 May 2012.
50. Nishikawa W, Tanaka I (eds). 1988 Precise Measurement Method for Complex Permittivity of Microwave Dielectric Substrate. In *Conf. on Precision Electromagnetic Measurements*, 7–10 June 1988.
51. Cullen AL, Yu PK, Barlow HEM. 1971 The accurate measurement of permittivity by means of an open resonator. *Proc. R. Soc. Lond. A Math. Phys. Sci.* **325**, 493–509. (doi:10.1098/rspa.1971.0181)
52. Suzuki H, Kamijo T. 2008 Millimeter-wave measurement of complex permittivity by perturbation method using open resonator. *IEEE Trans. Instrum. Meas.* **57**, 2868–2873. (doi:10.1109/TIM.2008.926448)
53. Clarke RN, Rosenberg CB. 1982 Fabry-Perot and open resonators at microwave and millimetre wave frequencies, 2–300 GHz. *J. Phys. E: Sci. Instrum.* **15**, 9–24. (doi:10.1088/0022-3735/15/1/002)
54. Cook RJ, Jones RG, Rosenberg CB. 1974 Comparison of cavity and open-resonator measurements of permittivity and loss angle at 35 GHz. *IEEE Trans. Instrum. Meas.* **23**, 438–442. (doi:10.1109/TIM.1974.4314330)
55. Yongliang Y, Hongling C, Junhu W, En L, Bingjie T (eds). 2014 Broadband measurement of complex permittivity by an open resonator at 20–40 GHz. In *IEEE Int. Conf. on Communiction Problem-solving*, 5–7 Dec. 2014.
56. Afsar MN, Hanyi D. 2001 A novel open-resonator system for precise measurement of permittivity and loss-tangent. *IEEE Trans. Instrum. Meas.* **50**, 402–405. (doi:10.1109/19.918152)
57. Bois KJ, Benally AD, Zoughi R. 1999 Multimode solution for the reflection properties of an open-ended rectangular waveguide radiating into a dielectric half-space: the forward and inverse problems. *IEEE Trans. Instrum. Meas.* **48**, 1131–1140. (doi:10.1109/19.816127)
58. Fallahpour M, Kajbaf H, Ghasr M, Case J, Zoughi R. 2012 Simultaneous evaluation of multiple key material properties of complex stratified structures with large spatial extent. *AIP Conf. Proc.* **1430**, 561–565. (doi:10.1063/1.4716277)
59. Lee C-K *et al.*. 2019 Evaluation of microwave characterization methods for additively manufactured materials. *Designs* **3**, 47.
60. Bakhtiari S, Qaddoumi N, Ganchev SI, Zoughi R. 1994 Microwave noncontact examination of disbond and thickness variation in stratified composite media. *IEEE Trans. Microwave Theory Tech.* **42**, 389–395. (doi:10.1109/22.277431)
61. Ganchev SI, Qaddoumi N, Bakhtiari S, Zoughi R. 1995 Calibration and measurement of dielectric properties of finite thickness composite sheets with open-ended coaxial sensors. *IEEE Trans. Instrum. Meas.* **44**, 1023–1029. (doi:10.1109/19.475149)
62. Grant JP, Clarke RN, Symm GT, Spyrou NM. 1989 A critical study of the open-ended coaxial line sensor technique for RF and microwave complex permittivity measurements. *J. Phys. E: Sci. Instrum.* **22**, 757–770. (doi:10.1088/0022-3735/22/9/015)
63. Davidovich M (eds). 2006 Inverse Problem Solution for Multilayered Waveguide and Coaxial Structures. In *Int. Conf. on Mathematical Methods in Electromagnetic Theory*, 26–29 June 2006.
64. Gao Y, Ghasr MT, Nacy M, Zoughi R. 2019 Towards accurate and wideband in vivo measurement of skin dielectric properties. *IEEE Trans. Instrum. Meas.* **68**, 512–524. (doi:10.1109/TIM.2018.2849519).
65. Bakhtiari S, Ganchev SI, Zoughi R. 1994 Analysis of radiation from an open-ended coaxial line into stratified dielectrics. *IEEE Trans. Microwave Theory Tech.* **42**, 1261–1267. (doi:10.1109/22.299765)
66. Ching-Lei L, Kun-Mu C. 1995 Determination of electromagnetic properties of materials using flanged open-ended coaxial probe-full-wave analysis. *IEEE Trans. Instrum. Meas.* **44**, 19–27. (doi:10.1109/19.368108)

67. Rocca P, Benedetti M, Donelli M, Franceschini D, Massa A. 2009 Evolutionary optimization as applied to inverse problems. *Inverse Prob.* **25**, 1–41. (doi:10.1088/0266-5611/25/12/123003)
68. Baker-Jarvis J, Janezic MD, Domich PD, Geyer RG. 1994 Analysis of an open-ended coaxial probe with lift-off for nondestructive testing. *IEEE Trans. Instrum. Meas.* **43**, 711–718. (doi:10.1109/19.328897)
69. Baker-Jarvis J. 1990 *Transmission/reflection and short-circuit line permittivity measurements: NIST technical note 1341*. Washington, DC: NIST.
70. Pozar DM. 2012 *Microwave engineering*, 4th edn. New York, NY: Wiley.
71. Gregory A, Clarke R, Hodgetts T, Symm G. 2008 RF and microwave dielectric measurements upon layered materials using coaxial sensors. Report no. DES125. See http://eprintspublications.npl.co.uk/334/1/des125.pdf.
72. Meaney PM, Gregory AP, Seppälä J, Lahtinen T. 2016 Open-ended coaxial dielectric probe effective penetration depth determination. *IEEE Trans. Microwave Theory Tech.* **64**, 915–923. (doi:10.1109/tmtt.2016.2519027)
73. Stuchly MA, Stuchly SS. 1980 Coaxial line reflection methods for measuring dielectric properties of biological substances at radio and microwave frequencies-a review. *IEEE Trans. Instrum. Meas.* **29**, 176–183. (doi:10.1109/TIM.1980.4314902)
74. Deming X, Liping L, Zhiyan J. 1987 Measurement of the dielectric properties of biological substances using an improved open-ended coaxial line resonator method. *IEEE Trans. Microwave Theory Tech.* **35**, 1424–1428. (doi:10.1109/TMTT.1987.1133870)
75. Neumayer M, Flatscher M, Bretterklieber T. 2019 Coaxial probe for dielectric measurements of aerated pulverized materials. *IEEE Trans. Instrum. Meas.* **68**, 1402–1411. (doi:10.1109/TIM.2019.2905710)
76. Mathur P, Thakur A, Augustine R, Kurup DG. (eds). 2019 A novel Non-Invasive Microwave Technique for monitoring Salinity in Water. In *TENCON 2019–2019 IEEE Region 10 Conf. (TENCON)*, 17–20 Oct. 2019.
77. Bakhtiari S, Ganchev SI, Zoughi R. 1993 Open-ended rectangular waveguide for nondestructive thickness measurement and variation detection of lossy dielectric slabs backed by a conducting plate. *IEEE Trans. Instrum. Meas.* **42**, 19–24. (doi:10.1109/19.206673)
78. Chih-Wei C, Kun-Mu C, Jian Q. 1997 Nondestructive determination of electromagnetic parameters of dielectric materials at X-band frequencies using a waveguide probe system. *IEEE Trans. Instrum. Meas.* **46**, 1084–1092. (doi:10.1109/19.676717)
79. Teodoridis V, Sphicopoulos T, Gardiol FE. 1985 The reflection from an open-ended rectangular waveguide terminated by a layered dielectric medium. *IEEE Trans. Microwave Theory Tech.* **33**, 359–366. (doi:10.1109/TMTT.1985.1133006)
80. Sanadiki BA, Mostafavi M. 1991 Inversion of inhomogeneous continuously varying dielectric profiles using open-ended waveguides. *R. Soc. Open Sci.* **39**, 158–163. (doi:10.1109/8.68177)
81. Ganchev SI, Bakhtiari S, Zoughi R. 1992 A novel numerical technique for dielectric measurement of generally lossy dielectrics. *IEEE Trans. Instrum. Meas.* **41**, 361–365. (doi:10.1109/19.153329)
82. Tantot O, Chatard-Moulin M, Guillon P. 1997 Measurement of complex permittivity and permeability and thickness of multilayered medium by an open-ended waveguide method. *IEEE Trans. Instrum. Meas.* **46**, 519–522. (doi:10.1109/19.571900)
83. Niu M, Su Y, Yan J, Fu C, Xu D. 1998 An improved open-ended waveguide measurement technique on parameters /spl epsiv//sub /spl gamma// and /spl mu//sub /spl gamma// of high-loss materials. *IEEE Trans. Instrum. Meas.* **47**, 476–481. (doi:10.1109/19.744194)
84. Faircloth DL, Baginski ME, Wentworth SM. 2006 Complex permittivity and permeability extraction for multilayered samples using S-parameter waveguide measurements. *IEEE Trans. Microwave Theory Tech.* **54**, 1201–1209. (doi:10.1109/TMTT.2005.864104)
85. Sanadiki B, Mostafavi M (eds). 1989 Inversion of multi-layer dielectrics using open-ended waveguides. In *Digest on Antennas and Propagation Society Int. Symp.*, 26–30 June 1989.
86. Ghasr MT, Simms D, Zoughi R. 2009 Multimodal solution for a waveguide radiating into multilayered structures—dielectric property and thickness evaluation. *IEEE Trans. Instrum. Meas.* **58**, 1505–1513. (doi:10.1109/TIM.2008.2009133)
87. Zoughi R, Gallion JR, Ghasr MT. 2016 Accurate microwave measurement of coating thickness on carbon composite substrates. *IEEE Trans. Instrum. Meas.* **65**, 951–953. (doi:10.1109/TIM.2016.2526698)

88. Lai J, Hughes D, Gallaher E, Zoughi R. (eds). 2004 Determination of the thickness and dielectric constant of a dielectric slab backed by free-space or a conductor through inversion of the reflection coefficient of a rectangular waveguide probe. In *Proc. of the 21st IEEE Instrumentation and Measurement Technology Conf. (IEEE Cat No04CH37510)*, 18–20 May 2004.
89. Croswell W, Taylor W, Swift C, Cockrell C. 1968 The input admittance of a rectangular waveguide-fed aperture under an inhomogeneous plasma: theory and experiment. *R. Soc. Open Sci.* **16**, 475–487. (doi:10.1109/TAP.1968.1139218)
90. Decreton MC, Gardiol FE. 1974 Simple nondestructive method for the measurement of complex permittivity. *IEEE Trans. Instrum. Meas.* **23**, 434–438. (doi:10.1109/TIM.1974.4314329)
91. Peer S, Case JT, Gallaher E, Kurtis KE, Zoughi R. 2003 Microwave reflection and dielectric properties of mortar subjected to compression force and cyclically exposed to water and sodium chloride solution. *IEEE Trans. Instrum. Meas.* **52**, 111–118. (doi:10.1109/TIM.2003.809099)
92. Case JT, Zoughi R, Donnell K, Hughes D, Kurtis KE. 2002 Microwave analysis of mortar prepared with type I/II, III and V cement and subjected to cyclical chloride exposure. *AIP Conf. Proc*. **615**, 498–505. (doi:10.1063/1.1472839)
93. Peer S, Zoughi R. 2004 Comparison of water and saltwater movement in mortar based on a semiempirical electromagnetic model. *IEEE Trans. Instrum. Meas.* **53**, 1218–1223. (doi:10.1109/TIM.2004.830741)
94. Bois KJ, Benally SD, Zoughi R. 2001 Near-field microwave non-invasive determination of NaCl in mortar. *IEE Proc.– Sci. Meas. Tech.* **148**, 178–182. (doi:10.1049/ip-smt:20010482)
95. Muñoz K, Akuthota B, Gallaher E, Zoughi R. 2004 Microwave reflection properties of mortar possessing a cyclically ingressed sodium chloride profile. *Mater. Eval.* **62**, 1049–1056.
96. Kempin M, Ghasr MT, Case JT, Zoughi R. 2014 Modified waveguide flange for evaluation of stratified composites. *IEEE Trans. Instrum. Meas.* **63**, 1524–1534. (doi:10.1109/TIM.2013.2291952)
97. Hasan AA (ed). 2013 Error analysis of rectangular waveguide probe with finite flange for nondestructive EM-properties and thickness measurement. In *IEEE INISTA*, 19–21 June 2013.
98. Karpisz T, Kopyt P, Salski B, Krupka J (eds). 2016 Open-ended waveguide measurement of liquids at millimeter wavelengths. In *2016 IEEE MTT-S International Microwave Symposium (IMS)*, 22–27 May 2016.
99. Afsar MN, Yong W, Hanyi D, Grignon R (eds). 2002 Measurement of complex permittivity of lossy liquids using open-ended waveguide technique. In *IEEE Antennas and Propagation Society International Symp. (IEEE Cat No02CH37313)*, 16–21 June 2002.
100. Hashemi A, Rashidi M, Kurtis KE, Donnell KM, Zoughi R. 2016 Microwave dielectric properties measurements of sodium and potassium water glasses. *Mater. Lett.* **169**, 10–12. (doi:10.1016/j.matlet.2015.11.036)
101. Julrat S, Trabelsi S (eds). 2018 Open-ended coplanar waveguide sensor for dielectric permittivity measurement. In *IEEE Int. Instrumentation and Measurement Technology Conference (I2MTC)*, 14–17 May 2018.
102. Hashemi A, Kurtis KE, Donnell KM, Zoughi R. 2017 Empirical multiphase dielectric mixing model for cement-based materials containing alkali-silica reaction gel. *IEEE Trans. Instrum. Meas.* **66**, 2428–2436. (doi:10.1109/TIM.2017.2707927)
103. Baker-Jarvis J, Vanzura EJ, Kissick WA. 1990 Improved technique for determining complex permittivity with the transmission/reflection method. *IEEE Trans. Microwave Theory Tech.* **38**, 1096–1103. (doi:10.1109/22.57336)
104. Lauer K, Wagner N, Felix-Henningsen P. 2012 A new technique for measuring broadband dielectric spectra of undisturbed soil samples. *Eur. J. Soil Sci.* **63**, 224–238. (doi:10.1111/j.1365-2389.2012.01431.x)
105. Schwing M, Chen Z, Scheuermann A, Wagner N (eds). 2014 Non-destructive coaxial transmission line measurements for dielectric soil characterization. In *IEEE Sensors Applications Symposium (SAS)*, 18–20 Feb. 2014.
106. Edwards CA, Donnell KM, Shearer CR (eds). 2018 Microwave materials characterization of geopolymer precursor powders. In *IEEE Int. Instrumentation and Measurement Technology Conference (I2MTC)*, 14–17 May 2018.
107. Havelka D, Krivosudský O, Cifra M. (eds). 2017 Grounded coplanar waveguide-based 0.5–50 GHz sensor for dielectric spectroscopy. In *47th European Microwave Conf. (EuMC)*, 17 10–12 Oct. 2017.

108. Bronckers LA, Smolders AB. 2016 Broadband Material Characterization Method Using a CPW With a Novel Calibration Technique. *IEEE Antennas Wirel. Propag. Lett.* **15**, 1763–1766. (doi:10.1109/LAWP.2016.2535115)
109. Jiqing H, Sligar A, Chih-Hung C, Shih-Lien L, Settaluri RK. 2006 A grounded coplanar waveguide technique for microwave measurement of complex permittivity and permeability. *IEEE Trans. Magn.* **42**, 1929–1931. (doi:10.1109/TMAG.2006.874098)
110. Das NK, Voda SM, Pozar DM. 1987 Two methods for the measurement of substrate dielectric constant. *IEEE Trans. Microwave Theory Tech.* **35**, 636–642. (doi:10.1109/TMTT.1987.1133722)
111. Toda AP, Flaviis FD. 2015 60-GHz substrate materials characterization using the covered transmission-line method. *IEEE Trans. Microwave Theory Tech.* **63**, 1063–1075. (doi:10.1109/TMTT.2015.2394740)
112. Ghodgaonkar DK, Varadan VV, Varadan VK. 1989 A free-space method for measurement of dielectric constants and loss tangents at microwave frequencies. *IEEE Trans. Instrum. Meas.* **38**, 789–793. (doi:10.1109/19.32194)
113. Rocha LS, Junqueira CC, Gambin E, Vicente AN, Culhaoglu AE, Kemptner E. (eds). 2013 A free space measurement approach for dielectric material characterization. In *SBMO/IEEE MTT-S Int. Microwave & Optoelectronics Conf. (IMOC)*, 4–7 Aug. 2013.
114. Trabelsi S, Nelson SO. 2003 Free-space measurement of dielectric properties of cereal grain and oilseed at microwave frequencies. *Meas. Sci. Technol.* **14**, 589–600. (doi:10.1088/0957-0233/14/5/308)
115. Chung J, Sertel K, Volakis JL. 2009 A non-invasive metamaterial characterization system using synthetic Gaussian aperture. *R. Soc. Open Sci.* **57**, 2006–2013. (doi:10.1109/TAP.2009.2021923)
116. Hajisaeid E, Dericioglu AF, Akyurtlu A. 2018 All 3-D printed free-space setup for microwave dielectric characterization of materials. *IEEE Trans. Instrum. Meas.* **67**, 1877–1886. (doi:10.1109/TIM.2018.2805962)
117. Gregory AP, Blackburn JF, Lees K, Clarke RN, Hodgetts TE, Hanham SM, Klein N. (eds). 2014 A near-field scanning microwave microscope for measurement of the permittivity and loss of high-loss materials. In *84th ARFTG Microwave Measurement Conf.*, 4–5 Dec 2014.
118. Jamal R, Olivier T, Nicolas D, Serge V. (eds). 2013 Non-destructive microwave characterization and imaging of dielectric materials using a near field technique. In *13th Mediterranean Microwave Symp. (MMS)*, 2–5 Sept. 2013.
119. Isakov D, Stevens CJ, Castles F, Grant PS. 2017 A split ring resonator dielectric probe for near-field dielectric imaging. *Sci. Rep.* 7, 2038. (doi:10.1038/s41598-017-02176-3)
120. Farina M, Donato AD, Mencarelli D, Venanzoni G, Morini A. 2012 High resolution scanning microwave microscopy for applications in liquid environment. *IEEE Microwave Compon. Lett.* **22**, 595–597. (doi:10.1109/LMWC.2012.2225607)
121. Lin T, Gu S, Lasri T. (eds). 2018 Resolution Improvement Method for Non-Destructive Imaging with Near-Field Scanning Microwave Microscopy. In *48th European Microwave Conf. (EuMC)*, 23–27 Sept 2018.
122. Gu S, Haddadi K, Fellahi AE, Lasri T. (eds). 2015 Near-field scanning microwave microscope for subsurface non-destructive characterization. In *European Microwave Conf. (EuMC)*, 7–10 Sept 2015.
123. Talanov VV, Scherz A, Moreland RL, Schwartz AR. 2006 Noncontact dielectric constant metrology of low-k interconnect films using a near-field scanned microwave probe. *Appl. Phys. Lett.* **88**, 192906. (doi:10.1063/1.2203238)
124. Rosner BT, van der Weide DW. 2002 High-frequency near-field microscopy. *Rev. Sci. Instrum.* **73**, 2505–2525. (doi:10.1063/1.1482150)
125. Wang Y, Bettermann AD, van der Weide DW. 2007 Process for scanning near-field microwave microscope probes with integrated ultratall coaxial tips. *J. Vac. Sci. Tech. B: Microelectron. Nanometer Struct. Process. Meas. Phenom.* **25**, 813–816. (doi:10.1116/1.2721571)
126. Álvarez LY, García Fernández M, Grau R, Las-Heras F. 2018 A synthetic aperture radar (SAR)-based technique for microwave imaging and material characterization. *Electronics* **7**, 1–15. (doi:10.3390/electronics7120373)
127. Gao Y, Qaseer MTA, Zoughi R. 2019 Complex Permittivity Extraction from Synthetic Aperture Radar (SAR) Images. *IEEE Trans. Instrum. Meas.* **1**, 4919–4929. (doi:10.1109/TIM.2019.2952479)

128. Fallahpour M, Baumgartner MA, Kothari A, Ghasr MT, Pommerenke D, Zoughi R. 2012 Compact Ka-Band one-port vector reflectometer using a wideband electronically controlled phase shifter. *IEEE Trans. Instrum. Meas.* **61**, 2807–2816. (doi:10.1109/TIM.2012.2196389)
129. Morales-Lovera H, Olvera-Cervantes J, Corona-Chavez A, Kataria TK. 2019 Dielectric anisotropy sensor using coupled resonators. *IEEE Trans. Microwave Theory Tech.* **68**, 1–7. (doi:10.1109/tmtt.2019.2958265)
130. Khadhra KB, Olk A, Gomez O, Fox A (eds). 2019 Permittivity estimation of rough dielectric surfaces by means of polarimetric bistatic measurements at millimeter wave frequencies. In *49th European Microwave Conf. (EuMC)*, 1–3 Oct 2019.
131. Barowski J, Jebramcik J, Wagner J, Pohl N, Rolfes I (eds). 2019 Spatial Identification of Dielectric Properties using Synthetic Aperture Radar. In *IEEE MTT-S International Microwave Workshop Series on Advanced Materials and Processes for RF and THz Applications (IMWS-AMP)*, 16–18 July 2019.
132. Xie Y, Meng Q, Xu K, Ran L, Wang J (eds). 2019 Far-field Characterization of Material Permittivity Based on Nonlinear Inversions. In *IEEE Int. Conf. on Computational Electromagnetics (ICCEM)*, 20–22 March 2019.
133. Chin-Yung Y, Reza Z. 1994 A novel microwave method for detection of long surface cracks in metals. *IEEE Trans. Instrum. Meas.* **43**, 719–725. (doi:10.1109/19.328896)
134. Kharkovsky S, Ghasr MT, Zoughi R. 2009 Near-field millimeter-wave imaging of exposed and covered fatigue cracks. *IEEE Trans. Instrum. Meas.* **58**, 2367–2370. (doi:10.1109/TIM.2009.2022380)
135. Yeh CY, Ranu E, Zoughi R. 1994 A novel microwave method for surface crack detection using higher order waveguide modes. *Mater. Eval.* **52**, 6.
136. Yeh C, Zoughi R. 1994 Microwave detection of finite surface cracks in metals using rectangular waveguides. *Res. Nondestr. Eval.* **6**, 35–55. (doi:10.1080/09349849409409679)
137. Yeh CY, Zoughi R. 1995 Sizing technique for slots and surface cracks in metals.
138. Ganchev SI, Zoughi R, Huber C, Runser RJ, Ranu E. 1996 Microwave method for locating surface slot/crack tips in metals. *Mater. Eval.* **54**, 5.
139. Huber C, Ganchev SI, Mirshahi R, Easter J, Zoughi R. 1997 remote detection of surface cracks/slots using open-ended rectangular waveguide sensors: an experimental investigation. *Nondestr. Testing Eval.* **13**, 227–237. (doi:10.1080/10589759708953032)
140. Huber C, Abiri H, Ganchev SI, Zoughi R. 1997 Analysis of the 'Crack characteristic signal' using a generalized scattering matrix representation. *IEEE Trans. Microwave Theory Tech.* **45**, 477–484. (doi:10.1109/22.566626)
141. Huber C, Abiri H, Ganchev SI, Zoughi R. 1997 Modeling of surface hairline-crack detection in metals under coatings using an open-ended rectangular waveguide. *IEEE Trans. Microwave Theory Tech.* **45**, 2049–2057. (doi:10.1109/22.644234)
142. Zoughi R, Ganchev SI, Huber C. 1998 Microwave measurement-parameter optimization for detection of surface breaking hairline cracks in metals. *Nondestr. Testing Eval.* **14**, 323–337. (doi:10.1080/10589759808953057)
143. Qaddoumi N, Ranu E, McColskey JD, Mirshahi R, Zoughi R. 2000 Microwave detection of stress-induced fatigue cracks in steel and potential for crack opening determination. *Res. Nondestr. Eval.* **12**, 87–104. (doi:10.1080/09349840009409652)
144. Ghasr MT, Kharkovsky S, Zoughi R, Austin R. 2005 Comparison of near-field millimeter-wave probes for detecting corrosion precursor pitting under paint. *IEEE Trans. Instrum. Meas.* **54**, 1497–1504. (doi:10.1109/TIM.2005.851086)
145. Gao Y, Ghasr MT, Ying K, Dvorsky M, Boots A, Zoughi R, Palmer D. (eds). 2019 Millimeter Wave Differential Probe System for Surface Crack Detection in Painted Aircraft Fuselage. In *IEEE Int. Instrumentation and Measurement Technology Conf. (I2MTC)*, 20–23 May 2019.
146. Ghasr MT, Carroll B, Kharkovsky S, Austin R, Zoughi R. 2006 Millimeter-wave differential probe for nondestructive detection of corrosion precursor pitting. *IEEE Trans. Instrum. Meas.* **55**, 1620–1627. (doi:10.1109/TIM.2006.880273)
147. McClanahan A, Kharkovsky S, Maxon AR, Zoughi R, Palmer DD. 2010 Depth evaluation of shallow surface cracks in metals using rectangular waveguides at millimeter-wave frequencies. *IEEE Trans. Instrum. Meas.* **59**, 1693–1704. (doi:10.1109/TIM.2009.2027780)
148. Kharkovsky S, McClanahan A, Zoughi R, Palmer DD. 2011 Microwave dielectric-loaded rectangular waveguide resonator for depth evaluation of shallow flaws in metals. *IEEE Trans. Instrum. Meas.* **60**, 3923–3930. (doi:10.1109/TIM.2011.2149370)

149. Gallion JR, Zoughi R. 2017 Millimeter-wave imaging of surface-breaking cracks in steel with severe surface corrosion. *IEEE Trans. Instrum. Meas.* **66**, 2789–2791. (doi:10.1109/TIM.2017.2735658)
150. Mazlumi F, Sadeghi SHH, Moini R. 2006 Interaction of rectangular open-ended waveguides with surface tilted long cracks in metals. *IEEE Trans. Instrum. Meas.* **55**, 2191–2197. (doi:10.1109/TIM.2006.884282)
151. Park HH, Cho YH, Eom HJ. 2001 Surface crack detection using flanged parallel-plate waveguide. *Electron. Lett.* **37**, 1526–1527. (doi:10.1049/el:20011051)
152. Campbell H. 2001 *Optimal open-ended waveguide probe design for surface crack detection in metals at microwave frequencies*. Fort Collins, CO: Colorado State University.
153. Qaddoumi N, Ganchev S, Zoughi R. (eds). 1994 A novel microwave fatigue crack detection technique using an open-ended coaxial line. In *Proc. of Conf. on Precision Electromagnetic Measurements Digest*, 27 June-1 July 1994.
154. Zoughi R, Hayes K, Ganchev SI. 1996 *Microwave detection of hairline surface-breaking cracks in metals using open-ended coaxial sensors: preliminary results*. SPIE.
155. Yang S-H, Kim K-B, Kang J-S. 2013 Detection of surface crack in film-coated metals using an open-ended coaxial line sensor and dual microwave frequencies. *NDT & E Int.* **54**, 91–95. (doi:10.1016/j.ndteint.2012.11.002)
156. Wang Y, Zoughi R. 2000 Interaction of surface cracks in metals with open ended coaxial probes at microwave frequencies. *Mater. Eval.* **58**, 1228–1234.
157. Wang N, Zoughi R. 2002 Moment method solution for modeling the interaction of open ended coaxial probes and surface cracks in metals. *Mater. Eval.* **60**, 1253–1258.
158. Donnell KM, McClanahan A, Zoughi R. 2014 On the crack characteristic signal from an open-ended coaxial probe. *IEEE Trans. Instrum. Meas.* **63**, 1877–1879. (doi:10.1109/TIM.2014.2317295)
159. Dong YD, Yang T, Itoh T. 2009 Substrate integrated waveguide loaded by complementary split-ring resonators and its applications to miniaturized waveguide filters. *IEEE Trans. Microwave Theory Tech.* **57**, 2211–2223. (doi:10.1109/TMTT.2009.2027156)
160. Albishi AM, Boybay MS, Ramahi OM. 2012 Complementary split-ring resonator for crack detection in metallic surfaces. *IEEE Microwave Compon. Lett.* **22**, 330–332. (doi:10.1109/LMWC.2012.2197384)
161. Albishi A, Ramahi O. 2014 Detection of surface and subsurface cracks in metallic and non-metallic materials using a complementary split-ring resonator. *Sensors (Basel, Switzerland).* **14**, 19 354–19 370. (doi:10.3390/s141019354)
162. Hu B, Ren Z, Boybay MS, Ramahi OM. 2014 Waveguide probe loaded with split-ring resonators for crack detection in metallic surfaces. *IEEE Trans. Microwave Theory Tech.* **62**, 871–878. (doi:10.1109/TMTT.2014.2309897)
163. Yun T, Lim S. 2014 High-Q and miniaturized complementary split ring resonator-loaded substrate integrated waveguide microwave sensor for crack detection in metallic materials. *Sens. Actuators, A.* **214**, 25–30. (doi:10.1016/j.sna.2014.04.006)
164. Ying K. 2017 *Application of millimeter-wave differential probe for crack detection on riveted structures*. Rolla, MO: Missouri University of Science and Technology.
165. Nadakuduti J, Genda C, Zoughi R. 2006 Semiempirical electromagnetic modeling of crack detection and sizing in cement-based materials using near-field microwave methods. *IEEE Trans. Instrum. Meas.* **55**, 588–597. (doi:10.1109/TIM.2006.870132)
166. Wang Y. 1999 *Modeling of surface crack detection using open-ended coaxial probes*. Fort Collins, CO: Colorado State University.
167. Pastorino M. 2010 *Microwave imaging vol. 208*. Hoboken, NJ: John Wiley & Sons.
168. Zoughi R. 2018 Microwave and millimeter wave nondestructive testing principles - back to basics. *Mater. Eval.* **76**, 1051–1057.
169. Case JT, Ghasr MT, Zoughi R. 2011 Optimum two-dimensional uniform spatial sampling for microwave SAR-based NDE imaging systems. *IEEE Trans. Instrum. Meas.* **60**, 3806–3815. (doi:10.1109/TIM.2011.2169177)
170. Tabib-Azar M, Pathak PS, Ponchak G, LeClair S. 1999 Nondestructive superresolution imaging of defects and nonuniformities in metals, semiconductors, dielectrics, composites, and plants using evanescent microwaves. *Rev. Sci. Instrum.* **70**, 2783–2792. (doi:10.1063/1.1149795)

171. Qaddoumi N, Bigelow T, Zoughi R, Brown L, Novack M. 2002 Reduction of sensitivity to surface roughness and slight standoff distance variations in microwave testing of thick composite structures. *Corpus* **60**, 165–170.
172. Kharkovsky S, Ryley AC, Stephen V, Zoughi R. 2008 Dual-polarized near-field microwave reflectometer for noninvasive inspection of carbon fiber reinforced polymer-strengthened structures. *IEEE Trans. Instrum. Meas.* **57**, 168–175. (doi:10.1109/TIM.2007.909497)
173. Kharkovsky S, Case JT, Abou-Khousa MA, Zoughi R, Hepburn FL. 2006 Millimeter-wave detection of localized anomalies in the space shuttle external fuel tank insulating foam. *IEEE Trans. Instrum. Meas.* **55**, 1250–1257. (doi:10.1109/TIM.2006.876543)
174. Ghasr MT *et al.*. 2011 Rapid rotary scanner and portable coherent wideband Q-band transceiver for high-resolution millimeter-wave imaging applications. *IEEE Trans. Instrum. Meas.* **60**, 186–197. (doi:10.1109/TIM.2010.2049216)
175. Case JT, Kharkovsky S, Zoughi R, Hepburn F. (eds). 2007 High Resolution Millimeter Wave Inspecting of the Orbiter Acreage Heat Tiles of the Space Shuttle. In *IEEE Instrumentation & Measurement Technology Conf. IMTC 2007*, 1–3 May 2007.
176. Henriksson T, Joachimowicz N, Conessa C, Bolomey J. 2010 Quantitative microwave imaging for breast cancer detection using a planar 2.45 GHz System. *IEEE Trans. Instrum. Meas.* **59**, 2691–2699. (doi:10.1109/TIM.2010.2045540)
177. Fallahpour M, Case JT, Ghasr MT, Zoughi R. 2014 Piecewise and Wiener Filter-based SAR techniques for monostatic microwave imaging of layered structures. *R. Soc. Open Sci.* **62**, 282–294. (doi:10.1109/TAP.2013.2287024)
178. Laviada J, Wu B, Ghasr MT, Zoughi R. 2019 Nondestructive evaluation of microwave-penetrable pipes by synthetic aperture imaging enhanced by full-wave field propagation model. *IEEE Trans. Instrum. Meas.* **68**, 1112–1119. (doi:10.1109/TIM.2018.2861078)
179. Wu B, Gao Y, Laviada J, Ghasr MT, Zoughi R. 2019 Time-reversal SAR imaging for nondestructive testing of circular and cylindrical multi-layered dielectric structures. *IEEE Trans. Instrum. Meas.* **1**, 2057–2066.
180. Franchois A, Joisel A, Pichot C, Bolomey J. 1998 Quantitative microwave imaging with a 2.45-GHz planar microwave camera. *IEEE Trans. Med. Imaging.* **17**, 550–561. (doi:10.1109/42.730400)
181. Ghasr MT, Abou-Khousa MA, Kharkovsky S, Zoughi R, Pommerenke D. 2012 Portable real-time microwave camera at 24 GHz. *R. Soc. Open Sci.* **60**, 1114–1125. (doi:10.1109/TAP.2011.2173145)
182. Ghasr MT, Kharkovsky S, Bohnert R, Hirst B, Zoughi R. 2013 30 GHz linear high-resolution and rapid millimeter wave imaging system for NDE. *R. Soc. Open Sci.* **61**, 4733–4740. (doi:10.1109/TAP.2013.2270174)
183. Ghasr MT, Case JT, Zoughi R. 2014 Novel reflectometer for millimeter-wave 3-D holographic imaging. *IEEE Trans. Instrum. Meas.* **63**, 1328–1336. (doi:10.1109/TIM.2014.2298618)
184. Ghasr MT, Horst MJ, Dvorsky MR, Zoughi R. 2017 Wideband microwave camera for real-time 3-D imaging. *R. Soc. Open Sci.* **65**, 258–268. (doi:10.1109/TAP.2016.2630598)
185. Laviada J, Ghasr MT, López-Portugués M, Las-Heras F, Zoughi R. 2018 Real-time multiview SAR imaging using a portable microwave camera with arbitrary movement. *R. Soc. Open Sci.* **66**, 7305–7314. (doi:10.1109/TAP.2018.2870485)
186. Horst MJ, Ghasr MT, Zoughi R. 2019 A compact microwave camera based on chaotic excitation synthetic-aperture radar. *R. Soc. Open Sci.* **67**, 4148–4161. (doi:10.1109/TAP.2019.2905712)
187. Kharkovsky S. 2013 Microwave Sensor Technologies for Structural Health Monitoring of Infrastructure. In *Second Conf. on Smart Monitoring, Assessment and Rehabilitation of Civil Structures (SMAR 2013)*, 9–11 Sept. 2013. Istanbul Technical University.
188. Kalantar-zadeh K. 2013 *Sensors: an introductory course*. Berlin, Germany: Springer.
189. Zhu C, Gerald RE, Chen Y, Huang J. 2019 Probing the theoretical ultimate limit of coaxial cable sensing: measuring nanometer-scale displacements. *IEEE Trans. Microwave Theory Tech.* **68**, 1–8. (doi:10.1109/tmtt.2019.2951099)
190. Sun S, Pommerenke DJ, Drewniak JL, Chen G, Xue L, Brower MA, Koledintseva MY. 2009 A novel TDR-based coaxial cable sensor for crack/strain sensing in reinforced concrete structures. *IEEE Trans. Instrum. Meas.* **58**, 2714–2725. (doi:10.1109/TIM.2009.2015706)

191. Wei T, Wu S, Huang J, Xiao H, Fan J. 2011 Coaxial cable Bragg grating. *Appl. Phys. Lett.* **99**, 113517. (doi:10.1063/1.3636406)
192. Huang J, Wei T, Lan X, Fan J, Xiao H. 2012 *Coaxial cable Bragg grating sensors for large strain measurement with high accuracy*. SPIE Smart Structures and Materials + Nondestructive Evaluation and Health Monitoring; 2012; San Diego, CA: SPIE.
193. Huang J, Wang T, Hua L, Fan J, Xiao H, Luo M. 2013 A coaxial cable Fabry-Perot interferometer for sensing applications. *Sensors (Basel, Switzerland)*. **13**, 15 252–15 260. (doi:10.3390/s131115252)
194. Cheng B, Yuan L, Zhu W, Song Y, Xiao H. 2017 A coaxial cable magnetic field sensor based on ferrofluid filled Fabry-Perot interferometer structure. *Sens. Actuators, A.* **257**, 194–197. (doi:10.1016/j.sna.2017.02.024)
195. Huang J, Lan X, Zhu W, Cheng B, Fan J, Zhou Z, Xiao H. 2016 Interferogram reconstruction of cascaded coaxial cable Fabry-Perot interferometers for distributed sensing application. *IEEE Sensors J.* **16**, 4495–4500. (doi:10.1109/JSEN.2016.2530839)
196. Zhu C, Chen Y, Zhuang Y, Huang J. 2018 Displacement and strain measurement up to 1000°C using a hollow coaxial cable Fabry-Perot resonator. *Sensors (Basel, Switzerland)*. **18**, 1304. (doi:10.3390/s18051304)
197. Ganchev SI, Qaddoumi N, Ranu E, Zoughi R. 1995 Microwave detection optimization of disbond in layered dielectrics with varying thickness. *IEEE Trans. Instrum. Meas.* **44**, 326–328. (doi:10.1109/19.377843)
198. Abou-Khousa M, Zoughi R. 2007 Disbond thickness evaluation employing multiple-frequency near-field microwave measurements. *IEEE Trans. Instrum. Meas.* **56**, 1107–1113. (doi:10.1109/TIM.2007.899848)
199. Donnell KM, Zoughi R. 2012 Detection of corrosion in reinforcing steel bars using microwave dual-loaded differential modulated scatterer technique. *IEEE Trans. Instrum. Meas.* **61**, 1–16. (doi:10.1109/TIM.2012.2200822)
200. Donelli M, Viani F. 2017 Remote inspection of the structural integrity of engineering structures and materials with passive MST Probes. *IEEE Trans. Geosci. Remote Sens.* **55**, 6756–6766. (doi:10.1109/TGRS.2017.2734042)
201. Capdevila S, Jofre L, Romeu J, Bolomey JC. 2013 Multi-loaded modulated scatterer technique for sensing applications. *IEEE Trans. Instrum. Meas.* **62**, 794–805. (doi:10.1109/TIM.2013.2240913)
202. Freiburger G, Zoughi R. (eds). 2005 Dielectric Material Characterization by Complex Ratio of Embedded Modulated Scatterer Technique States. In *IEEE Instrumentationand Measurement Technology Conf. Proc.*, 16–19 May 2005.
203. Donnell KM, Zoughi R. 2012 Application of embedded dual-loaded modulated scatterer technique (MST) to multilayer structures. *IEEE Trans. Instrum. Meas.* **61**, 2799–2806. (doi:10.1109/TIM.2012.2192355)
204. Hughes D, Zoughi R. (eds). 2003 Calculation of the impedance of a rectangular waveguide aperture in the presence of a loaded dipole antenna embedded in a generally lossy material. In *Proc. of the 20th IEEE Instrumentation Technology Conf. (Cat No03CH37412)*, 20–22 May 2003.
205. Hughes D, Zoughi R. 2005 A novel method for determination of dielectric properties of materials using a combined embedded modulated scattering and near-field microwave techniques-Part II: dielectric property recalculation. *IEEE Trans. Instrum. Meas.* **54**, 2398–2401. (doi:10.1109/TIM.2005.858133)
206. Joisel A, Bois KJ, Benally AD, Bolomey J-C, Zoughi R. 1999 *Embedded modulating dipole scattering for near-field microwave inspection of concrete: preliminary investigations*. SPIE's International Symposium on Optical Science, Engineering, and Instrumentation; 1999; Denver, CO: SPIE.
207. Bolomey J-C, Gardiol F. 2001 *Engineering applications of the modulated scatterer technique*. London, UK: Artech House.
208. Hughes D, Zoughi R. 2005 A novel method for determination of dielectric properties of materials using a combined embedded modulated scattering and near-field microwave techniques-Part I: forward model. *IEEE Trans. Instrum. Meas.* **54**, 2389–2397. (doi:10.1109/TIM.2005.858132)
209. Crocker DA, Donnell KM. 2015 Application of electrically invisible antennas to the modulated scatterer technique. *IEEE Trans. Instrum. Meas.* **64**, 3526–3535. (doi:10.1109/TIM.2015.2454671)

210. Brinker K, Zoughi R. (eds). 2018 Embedded chipless RFID measurement methodology for microwave materials characterization. In *IEEE International Instrumentation and Measurement Technology Conference (I2MTC)*, 14–17 May 2018.
211. Salama R, Kharkovsky S. (eds). 2013 An embeddable microwave patch antenna module for civil engineering applications. In *IEEE International Instrumentation and Measurement Technology Conference (I2MTC)*, 6–9 May 2013.
212. Tchafa FM, Huang H. 2019 Microstrip patch antenna for simultaneous temperature sensing and superstrate characterization. *Smart Mater. Struct.* **28**, 105009. (doi:10.1088/1361-665X/ab2213)
213. Sanders JW, Yao J, Huang H. 2015 Microstrip patch antenna temperature sensor. *IEEE Sensors J.* **15**, 5312–5319. (doi:10.1109/JSEN.2015.2437884)
214. Omer H, Azemi S, Abdullah Al-Hadi A, Soh PJ, Jamlos M. 2018 Structural health monitoring sensor based on A flexible microstrip patch antenna. *Indones. J. Electr. Eng. Comp. Sci.* **10**, 917–924. (doi:10.11591/ijeecs.v10.i3.pp917-924)
215. Herbko M, Lopato P. (eds). 2019 Sensitivity Analysis of Circular Microstrip Strain Sensor. In *International Interdisciplinary PhD Workshop (IIPhDW)*, 15–17 May 2019.
216. Qian Z, Tang Q, Li J, Zhao H, Zhang W. (eds). 2012 Analysis and design of a strain sensor based on a microstrip patch antenna. In *Int. Conf. on Microwave and Millimeter Wave Technology (ICMMT)*, 5–8 May 2012.
217. Yao J, Tjuatja S, Huang H. 2015 Real-time vibratory strain sensing using passive wireless antenna sensor. *IEEE Sensors J.***15**, 4338–4345. (doi:10.1109/JSEN.2015.2416672)
218. Bogosanovich M. 2000 Microstrip patch sensor for measurement of the permittivity of homogeneous dielectric materials. *IEEE Trans. Instrum. Meas.* **49**, 1144–1148. (doi:10.1109/19.872944)
219. Shams KMZ, Ali M, Miah AM. (eds). 2006 Characteristics of an Embedded Microstrip Patch Antenna for Wireless Infrastructure Health Monitoring. In *IEEE Antennas and Propagation Society Int. Symp.*, 9–14 July 2006.
220. Mohammad I, Gowda V, Zhai H, Huang H. 2011 Detecting crack orientation using patch antenna sensors. *Meas. Sci. Technol.* **23**, 015102. (doi:10.1088/0957-0233/23/1/015102)
221. Munk BA. 2005 *Frequency selective surfaces: theory and design*, 1st edn. New York, NY: Wiley-Interscience.
222. Pieper DF, Donnell KM. (eds). 2015 Approximation of effective dielectric constant for FSS in layered dielectrics using conformal mapping. In *IEEE Int. Symp. on Antennas and Propagation & USNC/URSI National Radio Science Meeting*, 19–24 July 2015.
223. Mahmoodi M, Donnell KM. (eds). 2017 Active frequency selective surface for strain sensing. In *IEEE Int. Symp. on Antennas and Propagation & USNC/URSI National Radio Science Meeting*, 9–14 July 2017.
224. Pieper D, Donnell KM, Abdelkarim O, ElGawady MA. (eds). 2016 Embedded FSS sensing for structural health monitoring of bridge columns. In *IEEE Int. Instrumentation and Measurement Technology Conf. Proc.*, 23–26 May 2016.
225. Suhaimi SA, Azemi SN, Jack SP. (eds). 2016 Structural Health Monitoring system using 3D frequency selective surface. In *IEEE Asia-Pacific Conf. on Applied Electromagnetics (APACE)*, 11–13 Dec 2016.
226. Mahmoodi M, Donnell KM. (eds). 2019 Improvement in FSS-Based Sensor Sensitivity by Miniaturization Technique. In *IEEE Int. Symp. on Antennas and Propagation and USNC-URSI Radio Science Meeting*, 7–12 July 2019.
227. Mahmoodi M, Donnell KM. (eds). 2017 Novel FSS-based sensor for concurrent temperature and strain sensing. In *IEEE Int. Symp. on Antennas and Propagation & USNC/URSI National Radio Science Meeting*, 9–14 July 2017.
228. Kinzel E. (eds). 2014 Design of a Frequency-Selective Surface strain sensor. In *IEEE Antennas and Propagation Society Int. Symp. (APSURSI)*, 6–11 July 2014.
229. Pieper DF, Donnell KM. (eds). 2015 Application of frequency selective surfaces for inspection of layered structures. In *IEEE Int. Instrumentation and Measurement Technology Conf. (I2MTC) Proc.*, 11–14 May 2015.
230. Jang S-D, Kang B-W, Kim J. 2012 Frequency selective surface based passive wireless sensor for structural health monitoring. *Smart Mater. Struct.* **22**, 025002. (doi:10.1088/0964-1726/22/2/025002)

231. Suhaimi S, Azemi S, Soh PJ. 2018 Feasibility study of frequency selective surfaces for structural health monitoring system. *Prog. Electromag. Res. C* 80, 199–209. (doi:10.2528/PIERC17081802)
232. Athauda T, Karmakar N. 2019 Chipped versus chipless RF identification: a comprehensive review. *IEEE Microwave Mag.* **20**, 47–57. (doi:10.1109/MMM.2019.2922118)
233. Preradovic S, Karmakar N. 2012 *Multiresonator-based chipless RFID barcode of the future*. Berlin, Germany: Springer.
234. Perret E. 2014 *Radio frequency identification and sensors: from RFID to chipless RFID*. Hoboken, NJ: Wiley.
235. Brinker K. 2019 Passively-Coded Embedded Microwave Sensors for Materials Characterization and Structural Health Monitoring (SHM). Master's, Missouri University of Science and Technology.
236. Brinker KR, Vaccaro M, Zoughi R. 2019 Application-adaptable Chipless RFID tag: design methodology, metrics, and measurements. *IEEE Trans. Instrum. Meas.* **69**, 1.
237. Martinez M, Weide Dvd (eds). 2017 Chipless RFID temperature threshold sensor and detection method. In *IEEE Int. Conf. on RFID (RFID), 9–11 May 2017*.
238. Khalifeh R, Yasri MS, Lescop B, Gallée F, Diler E, Thierry D, Rioual S. 2016 Development of wireless and passive corrosion sensors for material degradation monitoring in coastal zones and immersed environment. *IEEE J. Oceanic Eng.* **41**, 776–782. (doi:10.1109/JOE.2016.2572838)
239. Deif S, Harron L, Daneshmand M. (eds). 2018 Out-of-Sight Salt-Water Concentration Sensing Using Chipless- RFID for Pipeline Coating Integrity. In *IEEE/MTT-S Int. Microwave Symp. – IMS*, 10–15 June 2018.
240. Dey S, Karmakar NC (eds). 2015 Chipless RFID strain sensors: A novel feasibility analysis in terms of conventional patch antennas. In *IEEE MTT-S Int. Microwave and RF Conf. (IMaRC), 10–12 Dec. 2015*.
241. Occhiuzzi C, Paggi C, Marrocco G. 2011 Passive RFID strain-sensor based on meander-line antennas. *R. Soc. Open Sci.* **59**, 4836–4840. (doi:10.1109/TAP.2011.2165517)
242. Kim J, Wang Z, Kim WS. 2014 Stretchable RFID for wireless strain sensing with silver nano ink. *IEEE Sensors J.* **14**, 4395–4401. (doi:10.1109/JSEN.2014.2335743)
243. Genovesi S, Costa F, Borgese M, Dicandia FA, Monorchio A, Manara G. (eds). 2017 Chipless RFID sensor for rotation monitoring. In *IEEE Int. Conf. on RFID Technology & Application (RFID-TA)*, 20–22 Sept. 2017.
244. Perret E. (ed). 2017 Micrometrie displacement sensor based on chipless RFID. In *IEEE MTT-S Int. Microwave Symp. (IMS), 4–9 June 2017*.
245. Fan S, Chang T, Liu X, Fan Y, Tentzeris MM. (eds). 2018 A Depolarizing Chipless RFID Tag with Humidity Sensing Capability. In *IEEE Int. Symp. on Antennas and Propagation & USNC/URSI National Radio Science Meeting*, 8–13 July 2018.
246. Borgese M, Dicandia FA, Costa F, Genovesi S, Manara G. 2017 An Inkjet Printed Chipless RFID Sensor for Wireless Humidity Monitoring. *IEEE Sensors J.* **17**, 4699–4707. (doi:10.1109/JSEN.2017.2712190)
247. Marindra AMJ, Tian GY. 2018 Chipless RFID sensor tag for metal crack detection and characterization. *IEEE Trans. Microwave Theory Tech.* **66**, 2452–2462. (doi:10.1109/TMTT.2017.2786696)
248. Marindra AMJ, Sutthaweekul R, Tian GY. (eds). 2018 Depolarizing Chipless RFID Sensor Tag for Characterization of Metal Cracks Based on Dual Resonance Features. In *10th Int. Conf. on Information Technology and Electrical Engineering (ICITEE)*, 24–26 July 2018.
249. Kalansuriya P, Bhattacharyya R, Sarma S, Karmakar N. (eds). 2012 Towards chipless RFID-based sensing for pervasive surface crack detection. In *IEEE Int. Conf. on RFID-Technologies and Applications (RFID-TA)*, 5–7 Nov 2012.
250. Lázaro A, Villarino R, Costa F, Genovesi S, Gentile A, Buoncristiani L, Girbau D. 2018 Chipless dielectric constant sensor for structural health testing. *IEEE Sensors J.* **18**, 5576–5585. (doi:10.1109/JSEN.2018.2839689)
251. Costa F, Gentile A, Genovesi S, Buoncristiani L, Lazaro A, Villarino R, Girbau D. 2018 A depolarizing Chipless RF label for dielectric permittivity sensing. *IEEE Microwave Compon. Lett.* **28**, 371–373. (doi:10.1109/LMWC.2018.2820604)

252. Suwalak R, Phongcharoenpanich C, Torrungrueng D, Akkaraekthalin P. (eds). 2015 Dielectric material determination using the radar equation in RFID sensor applications. In *IEEE Conf. on Antenna Measurements & Applications (CAMA)*, 30 Nov-2 Dec. 2015.
253. Girbau D, Lázaro A, Villarino R. (eds). 2012 Passive wireless permittivity sensor based on frequency-coded chipless RFID tags. In *IEEE/MTT-S Int. Microwave Symp. Digest*, 17–22 June 2012.
254. Vena A, Tedjini M, Björninen T, Sydänheimo L, Ukkonen L, Tentzeris MM. (eds). 2014 A novel inkjet-printed wireless chipless strain and crack sensor on flexible laminates. In *IEEE Antennas and Propagation Society Int. Symp. (APSURSI)*, 6–11 July 2014.
255. Perret E. (ed.) 2016 Permittivity characterization based on Radar Cross measurements. In *URSI Int. Symp. on Electromagnetic Theory (EMTS)*, 14–18 Aug 2016.
256. Suwalak R, Lertsakwimarn K, Phongcharoenpanich C, Torrungrueng D. (eds) 2016 Dual-band chipless RFID sensor for a material quality monitoring application. In *Int. Symp. on Antennas and Propagation (ISAP)*, 24–28 Oct 2016.
257. Çetin E, Sahin MB. (eds). 2018 Array Strategies for Improving the Performances of Chipless RFID Tags. In *IEEE Int. Symp. on Antennas and Propagation & USNC/URSI National Radio Science Meeting*, 8–13 July 2018.
258. Koswatta R, Karmakar NC. (eds). 2010 Investigation into antenna performance on read range improvement of chipless RFID tag reader. In *Asia-Pacific Microwave Conf.*, 7–10 Dec 2010.
259. Rezaiesarlak R, Manteghi M. 2013 Short-time matrix pencil method for Chipless RFID detection applications. *R. Soc. Open Sci.* **61**, 2801–2806. (doi:10.1109/TAP.2013.2238497)
260. Anee R, Karmakar NC. 2013 Chipless RFID Tag Localization. *IEEE Trans. Microwave Theory Tech.* **61**, 4008–4017. (doi:10.1109/TMTT.2013.2282280)
261. Passafiume M, Collodi G, Cidronali A. (eds). 2019 Optimum Design of Low Energy Harvesting Detector at 5.8 GHz suitable for COTS devices. In *IEEE Int. Conf. on RFID Technology and Applications (RFID-TA)*, 25–27 Sept. 2019.
262. Yi J, Ki W, Tsui C. 2007 Analysis and design strategy of UHF micro-power cmos rectifiers for micro-sensor and RFID applications. *IEEE Trans. Circuits Syst. Regul. Pap.* **54**, 153–166. (doi:10.1109/TCSI.2006.887974)
263. Qi C, Frederick Q, Davis K, Lindsay D, Cox J, Parke S, Griffin JD, Durgin GD. (eds). 2018 A 5.8 GHz Energy Harvesting Tag for Sensing Applications in Space. In *6th IEEE Int. Conf. on Wireless for Space and Extreme Environments (WiSEE)*, 11–13 Dec 2018.
264. Ruan T, Chew ZJ, Zhu M. 2017 Energy-aware approaches for energy harvesting powered wireless sensor nodes. *IEEE Sensors J.* **17**, 2165–2173. (doi:10.1109/JSEN.2017.2665680)
265. Honda M, Sakurai T, Takamiya M. (eds). 2015 Wireless temperature and illuminance sensor nodes with energy harvesting from insulating cover of power cords for building energy management system. In *IEEE PES Asia-Pacific Power and Energy Engineering Conf. (APPEEC)*, 15–18 Nov 2015.
266. Brinker K, Zoughi R. (eds). 2019 Measurement of Inkjet-Printing Parameters for Accurate Chipless RFID Tag EM Simulation. In *IEEE Int. Instrumentation and Measurement Technologies Conf., Auckland, New Zealand*.
267. Islam MA, Karmakar NC. 2015 Real-world implementation challenges of a novel dual-polarized compact printable Chipless RFID Tag. *IEEE Trans. Microwave Theory Tech.* **63**, 4581–4591. (doi:10.1109/TMTT.2015.2495285)
268. Qi C, Amato F, Alhassoun M, Durgin GD. (eds). 2019 Breaking the range limit of RFID localization: phase-based positioning with tunneling tags. In *IEEE Int. Conf. on RFID (RFID), 2–4 April 2019*.
269. Khaliel M, El-Awamry A, Fawky A, Kaiser T. (eds). 2017 Long reading range chipless RFID system based on reflectarray antennas. In *11th European Conf. on Antennas and Propagation (EUCAP), 19–24 March 2017*.
270. Amato F, Peterson CW, Degnan BP, Durgin GD. 2018 Tunneling RFID Tags for long-range and low-power microwave applications. *IEEE J. Radio Frequency Identification.* **2**, 93–103. (doi:10.1109/JRFID.2018.2852498)
271. Jeong S, Hester JGD, Su W, Tentzeris MM. 2019 Read/interrogation enhancement of Chipless RFIDs using machine learning techniques. *IEEE Antennas Wirel. Propag. Lett.* **18**, 2272–2276. (doi:10.1109/LAWP.2019.2937055)
272. Karmakar N, Shrestha S, Bibile MA. 2017 TagID generation and detection of Chipless RFID system. *FERMAT.* **21**, Article 3.

273. Bardong J, Bruckner G, Kraft M, Fachberger R. (eds). 2009 Influence of packaging atmospheres on the durability of high-temperature SAW sensors. In *IEEE Int. Ultrasonics Symp., 20–23 Sept. 2009*.
274. Greve DW, Chin T-L, Zheng P, Ohodnicki P, Baltrus J, Oppenheim IJ. 2013 Surface acoustic wave devices for harsh environment wireless sensing. *Sensors (Basel, Switzerland)*. **13**, 6910–6935. (doi:10.3390/s130606910)
275. Rashidi M, Knapp MCL, Hashemi A, Kim J-Y, Donnell KM, Zoughi R, Jacobs LJ, Kurtis KE. 2016 Detecting alkali-silica reaction: a multi-physics approach. *Cem. Concr. Compos.* **73**, 123–135. (doi:10.1016/j.cemconcomp.2016.07.001)
276. De S, Gupta K, Joe Stanley R, Zoughi R, Doering K, Van Aken D, Steffes G, O'Keefe M, Palmer D. 2012 A comprehensive structural analysis process for failure assessment in aircraft lap-joint mimics using intramodal fusion of eddy current data. *Res. Nondestr. Eval.* **23**, 146–170. (doi:10.1080/09349847.2012.660242)